CHEMISTRY
A EUROPEAN JOURNAL

DOI: 10.1002/chem.200702013

Controlled Direct Synthesis of C-Mono- and C-Disubstituted Derivatives of $[3,3'\text{-}Co(1,2\text{-}C_2B_9H_{11})_2]^-$ with Organosilane Groups: Theoretical Calculations Compared with Experimental Results

Emilio José Juárez-Pérez,[a] Clara Viñas,[a] Arántzazu González-Campo,[a] Francesc Teixidor,[a] Reijo Sillanpää,[b] Raikko Kivekäs,[c] and Rosario Núñez*[a]

Abstract: Mono- and dilithium salts of $[3,3'\text{-}Co(1,2\text{-}C_2B_9H_{11})_2]^-$, ($\mathbf{1}^-$), react with different chlorosilanes (Me_2SiHCl, Me_2SiCl_2, Me_3SiCl and $MeSiHCl_2$) with an accurate control of the temperature to give a set of novel C_c-mono- ($C_c = C_{cluster}$) and C_c-disubstituted cobaltabis(dicarbollide) derivatives with silyl functions: $[1\text{-}SiMe_2H\text{-}3,3'\text{-}Co(1,2\text{-}C_2B_9H_{10})(1',2'\text{-}C_2B_9H_{11})]^-$ ($\mathbf{3}^-$); $[1,1'\text{-}\mu\text{-}SiMe_2\text{-}3,3'\text{-}Co(1,2\text{-}C_2B_9H_{10})_2]^-$ ($\mathbf{4}^-$); $[1,1'\text{-}\mu\text{-}SiMeH\text{-}3,3'\text{-}Co(1,2\text{-}C_2B_9H_{10})_2]^-$ ($\mathbf{5}^-$); $[1\text{-}SiMe_3\text{-}3,3'\text{-}Co(1,2\text{-}C_2B_9H_{10})(1',2'\text{-}C_2B_9H_{11})]^-$ ($\mathbf{6}^-$) and $[1,1'\text{-}(SiMe_3)_2\text{-}3,3'\text{-}Co(1,2\text{-}C_2B_9H_{10})_2]^-$ ($\mathbf{7}^-$). In a similar way, the $[8,8'\text{-}\mu\text{-}(1'',2''\text{-}C_6H_4)\text{-}1,1'\text{-}\mu\text{-}SiMe_2\text{-}3,3'\text{-}Co(1,2\text{-}C_2B_9H_9)_2]^-$ ($\mathbf{8}^-$); $[8,8'\text{-}\mu\text{-}(1'',2''\text{-}C_6H_4)\text{-}1,1'\text{-}\mu\text{-}SiMeH\text{-}3,3'\text{-}Co(1,2\text{-}C_2B_9H_9)_2]^-$ ($\mathbf{9}^-$) and $[8,8'\text{-}\mu\text{-}(1'',2''\text{-}C_6H_4)\text{-}1\text{-}SiMe_3\text{-}3,3'\text{-}Co(1,2\text{-}C_2B_9H_9)(1',2'\text{-}C_2B_9H_{10})]^-$ ($\mathbf{10}^-$) ions have been prepared from $[8,8'\text{-}\mu\text{-}(1'',2''\text{-}C_6H_4)\text{-}3,3'\text{-}Co(1,2\text{-}C_2B_9H_{10})_2]^-$ ($\mathbf{2}^-$). Thus, depending on the chlorosilane, the temperature and the stoichiometry of *n*BuLi used, it has been possible to control the number of substituents on the C_c atoms and the nature of the attached silyl function. All compounds were characterised by NMR and UV/Vis spectroscopy and MALDI-TOF mass spectrometry; $[NMe_4]$-**3**, $[NMe_4]$-**4** and $[NMe_4]$-**7** were successfully isolated in crystalline forms suitable for X-ray diffraction analyses. The $\mathbf{4}^-$ and $\mathbf{8}^-$ ions, which contain one bridging -μ-$SiMe_2$ group between each of the dicarbollide clusters, were unexpectedly obtained from the reaction of the monolithium salts of $\mathbf{1}^-$ and $\mathbf{2}^-$, respectively, with Me_2SiHCl at −78 °C in 1,2-dimethoxyethane. This suggests that an intramolecular reaction has taken place, in which the acidic C_c–H proton reacts with the hydridic Si–H, with subsequent loss of H_2. Some aspects of this reaction have been studied by using DFT calculations and have been compared with experimental results. In addition, DFT theoretical studies at the B3LYP/6-311G(d,p) level of theory were applied to optimise the geometries of ions $\mathbf{1}^-$–$\mathbf{10}^-$ and calculate their relative energies. Results indicate that the racemic mixtures, *rac* form, are more stable than the *meso* isomers. A good concordance between theoretical studies and experimental results has been achieved.

Keywords: carboranes · cluster compounds · density functional calculations · sandwich complexes · silanes

Introduction

In the last four decades, interest in the functionalisation and application of the cobaltabis(dicarbollide) ion $\mathbf{1}^-$ and its derivatives has grown due to their extraordinary chemical, thermal and radiation stability, and their similar properties to the inorganic superacids.[1] In addition, these compounds are hydrophobic[2,3] and weakly coordinating anions,[4] which have made them appropriate to be used as solid electrolytes,[3] strong non-oxidizing acids,[3] doping agents in conducting polymers[5] and extractants of radionuclides.[6] Cobaltabis(dicarbollide) derivative have also been used in diverse applications such as medical imaging and radiothera-

[a] E. J. Juárez-Pérez,[+] Prof. C. Viñas, Dr. A. González-Campo, Prof. F. Teixidor, Dr. R. Núñez
Institut de Ciència de Materials de Barcelona
CSIC, Campus U.A.B., 08193 Bellaterra (Spain)
Fax (+34) 935-805-729
E-mail: rosario@icmab.es

[b] Dr. R. Sillanpää
Department of Chemistry, University of Jyväskylä
40351, Jyväskylä (Finland)

[c] Prof. R. Kivekäs
Department of Chemistry, P.O. Box 55
University of Helsinki, 00014 (Finland)

[+] Emilio José Juárez-Pérez is enrolled in the Ph.D. program of the U.A.B.

py as boron-rich carriers for boron neutron capture therapy (BNCT).[7]

Many cobaltabis(dicarbollide) derivatives with substituents bonded to the cluster, preferably on the boron atoms, have been described.[8,9] However, there are few examples of C_c-substituted (C_c = cluster carbon atom) derivatives of $\mathbf{1}^-$ obtained directly from the deprotonation of C_c–H and subsequent attack by an electrophile. In 1997, Chamberlin et al. published a new synthetic method to bind methyl groups to the C_c atoms obtaining mono- and di-C_c-substituted cobaltabis(dicarbollide) derivatives.[10] More recently, we have reported the preparation of C_c-substituted cobaltabis(dicarbollide) derivatives with phosphine groups analogous to 2,2′-bis(diphenylphosphino)-1,1′-binaphthyl (BINAP) by the reaction of the dilithium salts of $\mathbf{1}^-$ with chlorodiarylphosphine in 1,2-dimethoxyethane (DME).[11]

Our interest in the synthesis and functionalisation of boron-rich dendrimeric structures containing carboranyl derivatives required us to develop new carboranylsilane compounds to use as molecular precursors and building blocks for the desired dendrimers, peripherally attached to carborane moieties.[12] Additionally, these carboranylsilane systems have been useful in the study of the reactivity of carborane derivatives towards different organosilanes and in testing them as hydrosilylating agents.[12a,b] In this work, we have extended our study to the cobaltabis(dicarbollide) anion due to its attractive properties and possible applications.[1–7] Special emphasis has been placed on bonding organosilane functions to the C atoms of the cluster to obtain previously unknown C_c-mono- and C_c-disubstituted cobaltabis(dicarbollide) derivatives with silyl groups. For this purpose, compounds have been prepared by the direct reaction of the lithium salts of $[3,3'\text{-Co}(1,2\text{-}C_2B_9H_{11})_2]^-$ ($\mathbf{1}^-$), and $[8,8'\text{-}\mu\text{-}(1'',2''\text{-}C_6H_4)\text{-}3,3'\text{-Co}(1,2\text{-}C_2B_9H_{10})_2]^-$ ($\mathbf{2}^-$), with different chlorosilanes. Some of these compounds have been proven to be active as hydrosilylating agents and can be used to functionalise different generations of dendrimers. Additionally, a theoretical study, using B3LYP density functional methods at the 6-311G(d,p) basis has provided remarkable data on conformational habits and relative energies of the metallacarborane reported here. The discussion is completed with the X-ray crystal structures of $[NMe_4][1\text{-}SiMe_2H\text{-}3,3'\text{-Co}(1,2\text{-}C_2B_9H_{10})(1',2'\text{-}C_2B_9H_{11})]$, $[NMe_4][1,1'\text{-}\mu\text{-}SiMe_2\text{-}3,3'\text{-Co}(1,2\text{-}C_2B_9H_{10})_2]$ and $[NMe_4][1,1'\text{-}(SiMe_3)_2\text{-}3,3'\text{-Co}(1,2\text{-}C_2B_9H_{10})_2]$.

Results and Discussion

Synthesis of C_c-substituted cobaltabis(dicarbollide) derivatives with silyl groups: With the goal of preparing a C_c-monosubstituted cobaltabis(dicarbollide) derivatives functionalised with the silyl group $-SiMe_2H$, the metallation of Cs-$[3,3'\text{-Co}(1,2\text{-}C_2B_9H_{11})_2]$ (Cs-**1**), with one equivalent of *n*-butyllitium (*n*BuLi) followed by the reaction with Me_2SiHCl (Me = methyl) in 1,2-dimethoxyethane at −78 °C for 1 h was performed. The resulting orange residue was dissolved in MeOH to yield, after precipitation with an aqueous solution of $[NMe_4]Cl$, a mixture of salts, which according to the ^1H and ^{11}B NMR spectra correspond to unreacted starting material $\mathbf{1}^-$ together with the monosubstituted $[1\text{-}SiMe_2H\text{-}3,3'\text{-Co}(1,2\text{-}C_2B_9H_{10})(1',2'\text{-}C_2B_9H_{11})]^-$ ($\mathbf{3}^-$), and $[1,1'\text{-}\mu\text{-}SiMe_2\text{-}3,3'\text{-Co}(1,2\text{-}C_2B_9H_{10})_2]^-$, ($\mathbf{4}^-$), obtained in 51 and 18%, respectively (Scheme 1). Attempts to separate these compounds by silica or alumina column chromatography were unsuccessful and led to $\mathbf{1}^-$ in all cases. The compound $[NMe_4]$-**3** was isolated in 11% yield after recrystallisation from CH_2Cl_2. The $\mathbf{3}^-$ ion was uniquely obtained when the reaction was carried out at −78 °C. At higher temperatures (e.g. −40 or 0 °C) or by using other solvents, such as THF, $\mathbf{3}^-$ was not formed. Crystals of $[NMe_4]$-**3** were obtained by slow evaporation of the compound in a mixture of acetone and water. The anion $\mathbf{3}^-$ represents the first example of a C_c-monosubstituted cobalta(bisdicarbollide) derivative that has been fully characterised by X-ray diffraction.

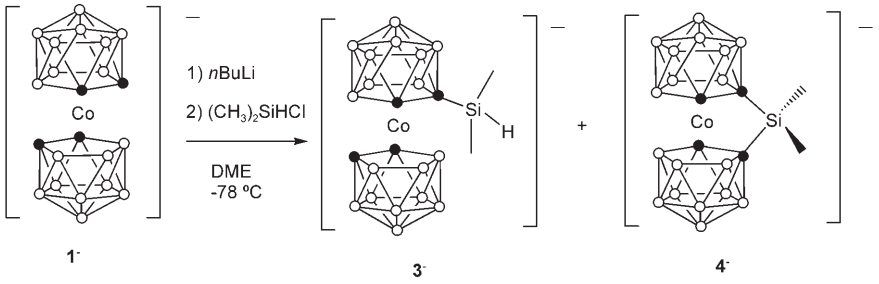

Scheme 1. Synthesis of ions $\mathbf{3}^-$ and $\mathbf{4}^-$.

The unexpected synthesis of $\mathbf{4}^-$ motivated us to study its synthesis in more detail. Two different strategies were used (Scheme 2): 1) the reaction of Cs-**1** with one equivalent of *n*BuLi at −40 °C in DME, followed by the reaction with an excess of Me_2SiHCl gave, after 3 h at room temperature, $[Li(dme)_2]$-**4**, according to the ^1H NMR spectrum; and 2) the reaction of Cs-**1** with 2 equivalents of *n*BuLi at −78 °C in DME, followed by the reaction with Me_2SiCl_2, gave the same species $[Li(dme)_2]$-**4**. The $\mathbf{4}^-$ ion could be isolated by using cations such as $[NMe_4]^+$, Cs^+ and $[PMe(Ph)_3]^+$ (Ph = phenyl) by dissolving $[Li(dme)_2]$-**4** in MeOH and adding aqueous solutions of $[NMe_4]Cl$, CsCl or a methanolic solution of $[PMe(Ph)_3]Br$ to yield the corresponding salts of $\mathbf{4}^-$ in 45, 62, and 70% yield, respectively. When $\mathbf{4}^-$ was synthesised at −40 °C, a mixture of structural isomers (as will be described in depth in a later section) was obtained as shown by the $^{11}B\{^1H\}$ NMR spectrum. However, at −78 °C mainly one isomer was formed. Monocrystals of $[NMe_4]$-**4** were ob-

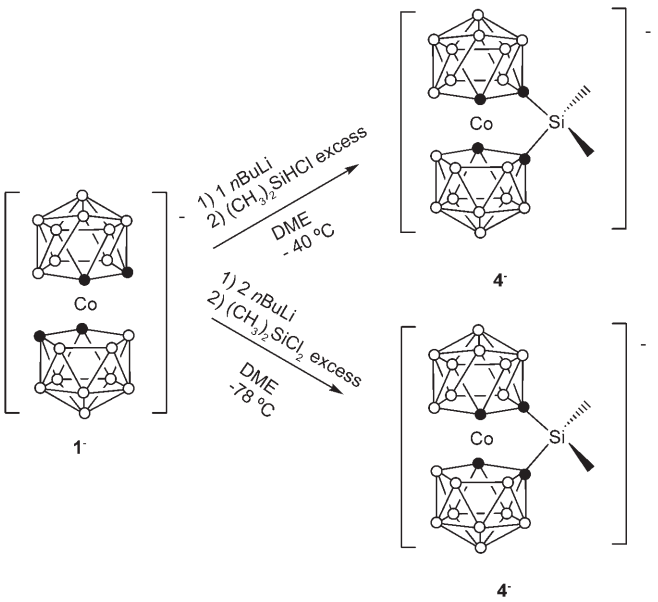

Scheme 2. Synthesis of ion $\mathbf{4}^-$ using two different approaches.

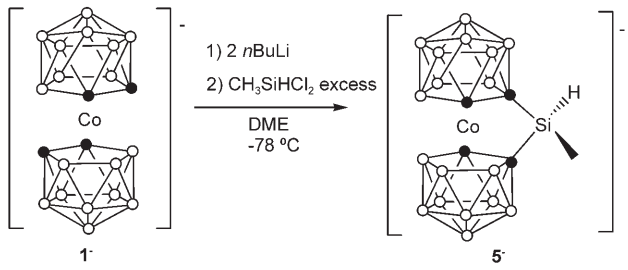

Scheme 3. Synthesis of the ion $\mathbf{5}^-$.

tained by slow evaporation of a solution of the compound synthesised at −40 °C in acetone.

As already mentioned, an attempt to get C_c-monosubstitution on cobaltabis(dicarbollide) with a group containing the −SiH function with $SiMe_2HCl$ led to $\mathbf{3}^-$ in low yield. As we were interested in the reactivity of a Si−H-containing cobaltabis(dicarbollide) derivative, we used $MeSiHCl_2$ as a chlorosilane source (Scheme 3). Cs-**1** was treated with two equivalents of *n*BuLi at −78 °C in DME followed by an excess of $MeSiHCl_2$ at the same temperature. Then, after stirring for 6 h at room temperature, the solution was evaporated and the residue treated with MeOH. The anion $\mathbf{5}^-$ was isolated as the Cs salt in 76% yield by precipitation with an aqueous solution of CsCl. The temperature of −78 °C used in this reaction was a key factor to produce $\mathbf{5}^-$ in 95% isomeric purity, according to the NMR spectra. The use of higher temperatures caused the formation of a mixture of structural isomers (see later section) along with unreacted starting material $\mathbf{1}^-$.

To learn about the reactivity of $\mathbf{1}^-$ towards chlorosilanes, its mono- and dilithium salts were treated with an excess of Me_3SiCl at −78 °C in DME. The monolithium salt of $\mathbf{1}^-$ led to a mixture of products, from which the C_c-monosubstituted [NMe_4]-**6** was isolated in 33% yield. Conversely, the dilithium salt gave the C_c-disubstituted $\mathbf{7}^-$, which was isolated as the [NMe_4]-**7** and Cs-**7** salts in 91 and 90% yield, respectively. Red crystals of [NMe_4]-**7** were successfully obtained from acetone. Metallacarboranes $\mathbf{6}^-$ and $\mathbf{7}^-$ were very convenient to interpret spectroscopic data and to get information about the possible rotational isomers in related compounds.

Silyl-functionalised derivatives of the rigid Cs[8,8′-μ-(1″,2″-C_6H_4)-3,3′-Co(1,2-$C_2B_9H_{10}$)$_2$] compound (Cs-**2**) with chlorosilanes were also studied. The reaction of Cs-**2** with one equivalent of *n*BuLi at −78 °C in DME, followed by the reaction with chlorodimethylsilane (Me_2SiHCl), led uniquely to [8,8′-μ-(1″,2″-C_6H_4)-1,1′-μ-$SiMe_2$-3,3′-Co(1,2-$C_2B_9H_9$)$_2$]$^-$ ($\mathbf{8}^-$; Scheme 4), which was isolated as a red solid in 77% yield by precipitation with an aqueous solution of [NMe_4]Cl. The spectroscopic study of [NMe_4]-**8**, which will be discussed later, indicated that $\mathbf{2}^-$ behaves similarly to homologous $\mathbf{1}^-$ with Me_2SiHCl. However, the formation of a C_c-monosubstituted species analogous to $\mathbf{3}^-$ was never observed, even at very low temperatures. Likewise, Cs-**2** was treated with two equivalents of *n*BuLi at −78 °C in DME and subsequently with an excess of $MeSiHCl_2$ to give $\mathbf{9}^-$ (Scheme 4). After

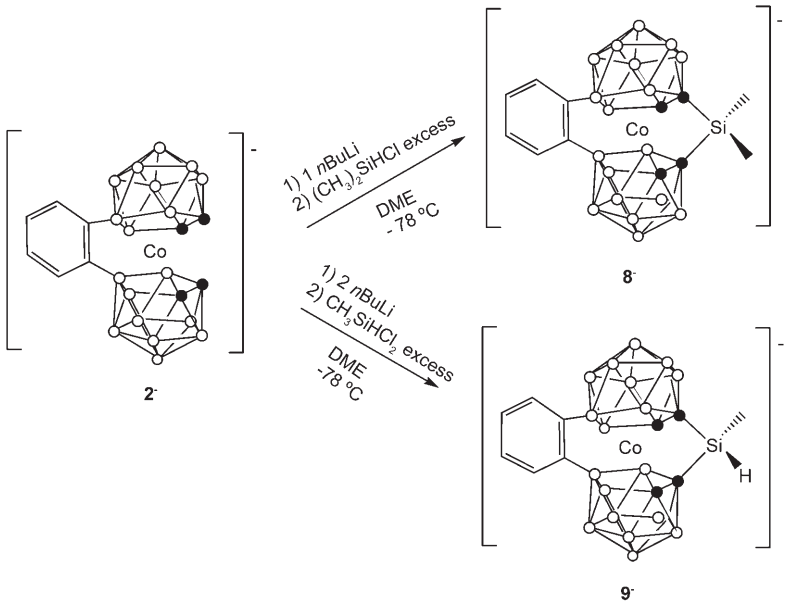

Scheme 4. Synthesis of cobaltabis(dicarbollide) ions $\mathbf{8}^-$ and $\mathbf{9}^-$.

their workup, the compounds [NMe_4]-**9** and Cs-**9** were isolated in 60 and 65% yield, respectively, by precipitation with aqueous solutions of [NMe_4]Cl and CsCl, respectively (Scheme 4).

Similarly, Cs-**2** was treated with two equivalents of *n*BuLi at −78°C in DME followed by an excess of Me_3SiCl under the same conditions to give mainly the monosubstituted compound [NMe_4]-**10** in 69% yield by precipitation with an aqueous solution of [NMe_4]Cl.

These results show that C_c-silyl derivatives of cobaltabis(dicarbollide) can be produced in good yields. The metallacarboranes containing the Si–H function are potential hydrosilylation agents and can be used to functionalise dendrimeric structures.

Characterisation of functionalised cobaltabis(dicarbollide) derivatives with silyl groups: All of the compounds described above were characterised by elemental analysis; UV/Vis, FTIR, and ^1H, ^{13}C, ^{11}B, and ^{29}Si NMR spectroscopy and matrix-assisted laser desorption ionisation time of flight (MALDI-TOF) mass spectrometry. In addition the compounds [NMe_4]-**3**, [NMe_4]-**4** and [NMe_4]-**7** were unequivocally confirmed by X-ray diffraction analysis.

Spectroscopic data: The ^1H, ^{11}B, ^{13}C and ^{29}Si NMR spectra of the products reported here agree with the structures proposed in the schemes. The IR spectra of all compounds present typical ν(B–H) strong bands for *closo*-clusters between 2554 and 2577 cm^{-1} and, additionally, intense bands in the region of 1250–1257 cm^{-1} corresponding to δ(Si–CH_3). Complexes **3**$^-$, **5**$^-$ and **9**$^-$ show a characteristic band near 2160 cm^{-1} attributed to ν(Si–H). The $^1H\{^{11}B\}$ NMR spectra of compounds **3**$^-$ and **5**$^-$ exhibit resonances at 4.31 and 5.06 ppm, respectively, which can be assigned to the Si–H function (Figure 1, Table 1). However, **9**$^-$ shows two resonances at 4.97 and 5.25 ppm with different areas. Both peaks can be attributed to the Si–H proton, indicating the presence of structural isomers in the solution, (see later). Moreover, **3**$^-$, **5**$^-$ and **9**$^-$ have a ^3J(H,H) = 3.4 Hz due to Si–H coupling with the protons on CH_3 and giving a quartet for **5**$^-$ and **9**$^-$ and a septet for **3**$^-$ (Figure 1). The corresponding

Table 1. Chemical shift values [ppm] of the selected protons in the ^1H NMR spectra of C_c-substituted derivatives **3**$^-$–**10**$^-$ and the starting ions **1**$^-$ and **2**$^-$.

	δ ^1H NMR			
	Si–H	C_c–H	Si–CH_3	B–H
1$^-$	–	3.94	–	3.37–1.57
3$^-$	4.31	3.85, 3.69	0.29	3.61–1.60
4$^-$	–	4.50	0.31	3.38–1.43
5$^-$	5.06	4.59	0.44	3.40–1.44
6$^-$	–	4.02, 3.83, 3.72	0.28	3.57–1.50
7$^-$	–	4.19, 3.77	0.33, 0.30	3.98–1.58
2$^-$	–	3.58	-	3.76–1.49
8$^-$	–	3.48	0.39, 0.25	4.00–1.43
9$^-$	5.25, 4.97	3.61	0.48, 0.38	4.11–1.43
10$^-$	–	3.52, 3.45	0.28	3.99–1.51

Si–CH_3 protons are exhibited at a higher field in the region 0.25–0.48 ppm (Table 1). These resonances appear as a doublet for **3**$^-$, **5**$^-$ and **9**$^-$, a singlet for **4**$^-$ (Figure 2) and two different singlets for its homologous **8**$^-$ due to the presence of structural isomers. Due to their symmetry, compounds **4**$^-$, **5**$^-$, **8**$^-$ and **9**$^-$ have only one resonance attributed to the C_c–H protons, while **7**$^-$ shows two signals in different ratios, indicating the presence of geometrical isomers. The C_c-monosubstituted **3**$^-$, **6**$^-$ and **10**$^-$ exhibit two resonances for C_c–H

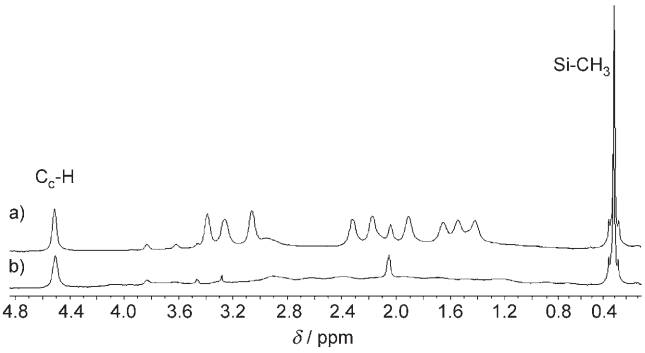

Figure 2. a) $^1H\{^{11}B\}$-NMR spectrum of Cs-**4** and b) ^1H NMR spectrum of Cs-**4**.

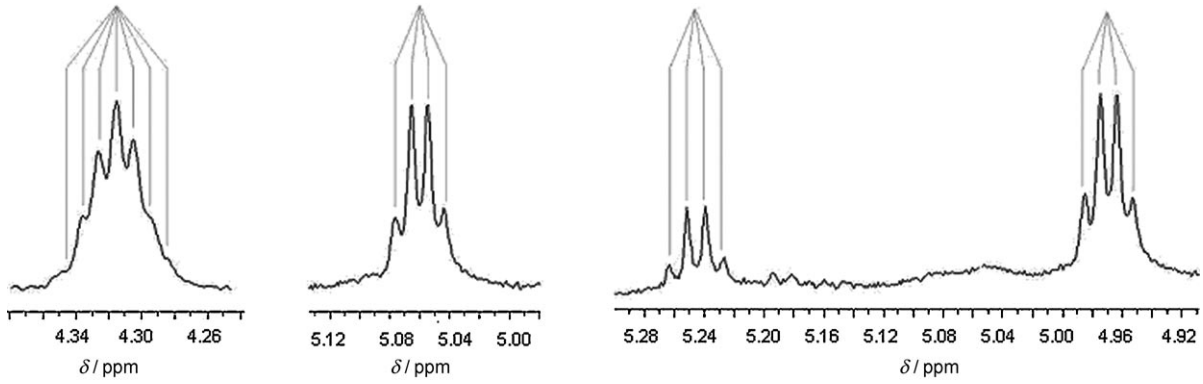

Figure 1. A portion of the ^1H NMR spectra corresponding to the Si–H protons chemical shifts in compounds: **3**$^-$ (left), **5**$^-$ (middle) and **9**$^-$ (right) with relative composition of 24 and 76% for the two structural isomers.

protons, one assigned to the substituted cluster and the second from the unsubstituted cluster (Table 1). The cluster B–H protons appear in the region ranging from 1.43–4.11 ppm (Table 1). In the $^{1}H\{^{11}B\}$ NMR spectrum of $\mathbf{4}^{-}$, nine resonances attributed to the nine B–H protons of each cluster are clearly observed (Figure 2a). The $^{13}C\{^{1}H\}$ NMR spectra show low intensity peaks in a wide region between 31.88 and 55.86 ppm. These high field C_c atoms can be assigned to the C_c–Si atoms. Resonances for the carbon atoms in the Si–CH_3 groups are high field, from 3.20 to −6.87 ppm. The $^{11}B\{^{1}H\}$ NMR spectra of ions $\mathbf{3}^{-}$–$\mathbf{7}^{-}$ display bands in a typical range from +9.1 to −22.3 ppm, indicative of *closo* species with all boron atoms in non-equivalent vertices. However, the resonances for boron atoms in $\mathbf{8}^{-}$, $\mathbf{9}^{-}$ and $\mathbf{10}^{-}$ appear between +27.5 and −24.5 ppm with a 2:6:4:4:2 pattern. In this case, the low-field resonance does not split in the ^{11}B NMR spectrum, which is attributed to the B8 atoms bonded to the phenyl group. Figure 3 shows a schematic representation of the $^{11}B\{^{1}H\}$ NMR spectra for $\mathbf{4}^{-}$ and $\mathbf{5}^{-}$ along with their precursor $\mathbf{1}^{-}$. Bands assignment has been done using a bidimensional COSY $^{11}B\{^{1}H\}/^{11}B\{^{1}H\}$ spectrum. In general, the presence of the silyl substituent at the C_c atoms shifts the ^{11}B resonances downfield with respect to the precursor. For $\mathbf{4}^{-}$, the resonances due to B4, 4′, 7, 7′, 9, 9′, 12, 12′ and B5, 5′, 11, 11′, which appear as two resonances of intensity 8 and 4 in $\mathbf{1}^{-}$, have evolved to three resonances of intensity 4, 2 and 2 and two resonances of intensity 2 due to the lost of symmetry. For $\mathbf{5}^{-}$, the presence of two different groups on the Si atom (CH_3 and H) causes higher asymmetry in the molecule, and this is reflected in the ^{11}B NMR spectrum. In addition, the $^{11}B\{^{1}H\}$ NMR spectrum of $\mathbf{3}^{-}$ shows a 1:1:1:1:1:4:3:2:2:1:1 pattern in the range from +9.10 to −22.26 ppm, while $\mathbf{6}^{-}$ exhibits a 1:1:1:1:1:1:2:2:2:1:1:1:1:1:1 pattern in the region of +8.20 to −23.00 ppm. Both spectra show a large number of resonances due to the loss of any symmetry operation besides E. Figure 4a displays the bidimensional $^{11}B\{^{1}H\}/^{11}B\{^{1}H\}$2D

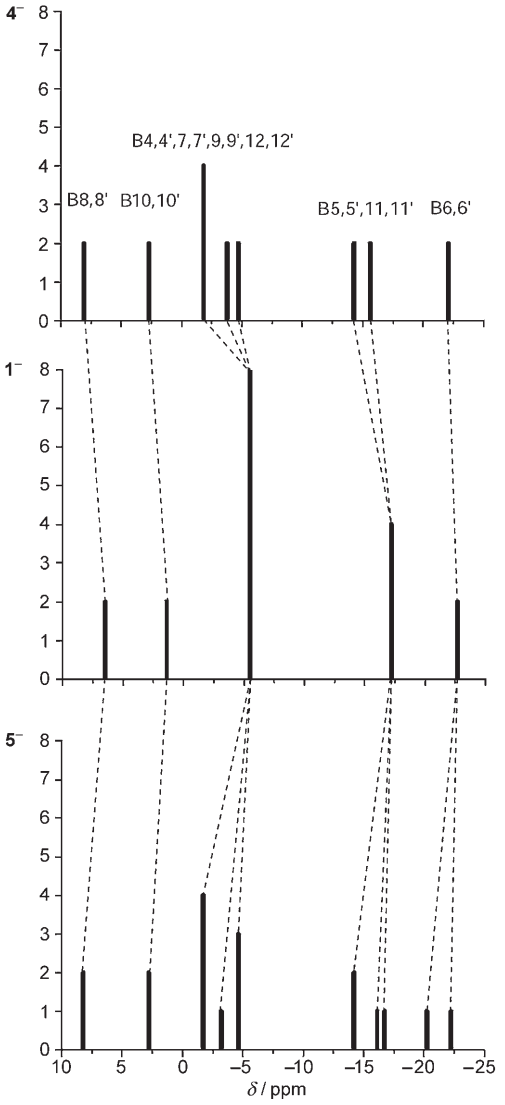

Figure 3. Stick representation of the chemical shifts and relative intensities in the $^{11}B\{^{1}H\}$ NMR spectra of some selected compounds.

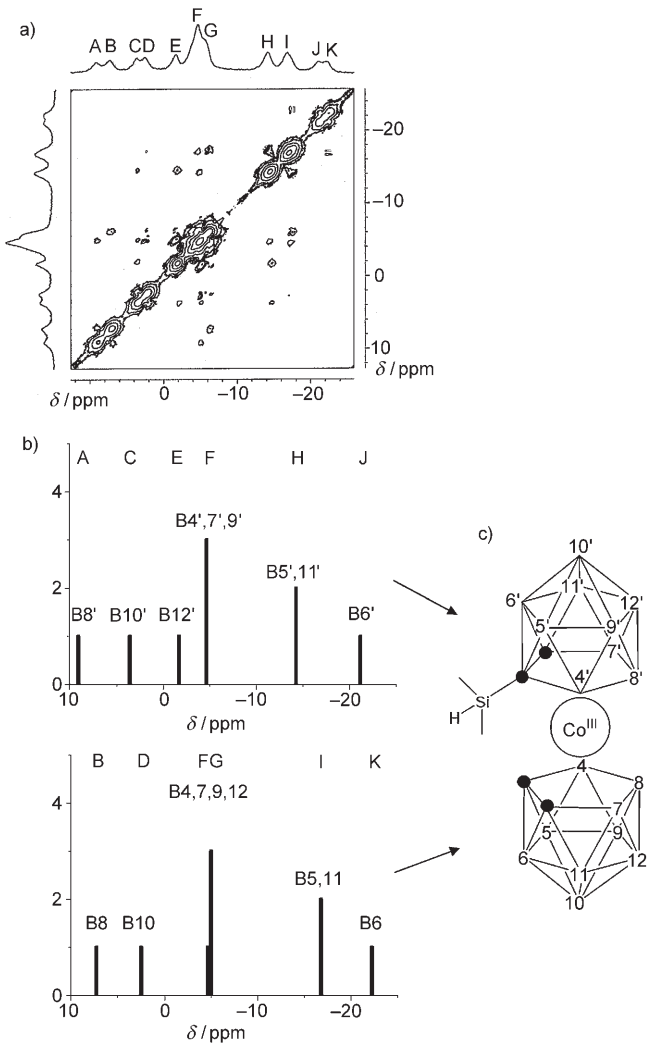

Figure 4. a) $^{11}B\{^{1}H\}$-$^{11}B\{^{1}H\}$2D COSY NMR spectrum of $\mathbf{3}^{-}$. b) Stick representation of the $^{11}B\{^{1}H\}$ NMR spectra of each dicarbollide ligand in $\mathbf{3}^{-}$. c) Schematic representation of the anion $\mathbf{3}^{-}$.

COSY NMR spectrum of $\mathbf{3}^-$ in which the resonances have been assigned to the corresponding boron atoms.[13] The spectrum has been assigned on the basis that each dicarbollide moiety behaves independently of the second.[14] These independent spectra are represented as stick diagrams in Figure 4b with the non-substituted ligand (lower diagram) and the substituted ligand (upper diagram). The combination of both produces a realistic image of the experimental spectrum. The ^{29}Si NMR spectra exhibit peaks in the range of 13.98 to −8.28 ppm (Table 2). The ^{29}Si chemical shifts are dependent on the substituents at the Si atom. The high-field (−8.28 ppm) signal is due to the $-SiMe_2H$ group in $\mathbf{3}^-$, and the corresponding resonances in $\mathbf{5}^-$ and $\mathbf{9}^-$ appear at 2.94 and 2.69 ppm, respectively. The Si atoms of the $-SiMe_3$ and bridging $-SiMe_2$ groups appear at a low field, between 10.75 and 13.98 ppm. Formulas of all the compounds were established by using MALDI-TOF mass spectrometry in the negative-ion mode without a matrix. Figure 5a displays the MALDI-TOF mass spectrum of the [1,1′-μ-SiMeH-3,3′-Co(1,2-$C_2B_9H_{10})_2$]$^-$ ion ($\mathbf{5}^-$) in which the molecular ion peak appears at $m/z = 366.2$ with a perfect concordance with the calculated pattern (Figure 5b). For all anions, a full agreement between the experimental and calculated patterns was also obtained for the molecular ion peaks. Thus, for $\mathbf{3}^-$, $\mathbf{6}^-$ and $\mathbf{10}^-$, this technique shows the corresponding molecular ion peaks at $m/z = 382.2$, 396.3 and 369.2, respectively, which agrees with the proposed structures.

Table 2. Chemical shift values [ppm] of the silicon nuclei in the ^{29}Si NMR spectrum of C_c-substituted cobaltabis(dicarbollides).

Compound	δ ^{29}Si	Compound	δ ^{29}Si
$\mathbf{3}^-$	−8.28	$\mathbf{7}^-$	10.75
$\mathbf{4}^-$	13.98	$\mathbf{8}^-$	11.74
$\mathbf{5}^-$	2.94	$\mathbf{9}^-$	2.69
$\mathbf{6}^-$	10.74	$\mathbf{10}^-$	8.63

UV/Vis spectra: The UV/Vis spectra of $\mathbf{1}^-$ and several *exo*-skeletal derivatives in different solvents such as methanol, but mostly in acetonitrile have been reported in different publications.[9j,15] There are some differences in the positions and absorption coefficients of the maxima, indicating that these values are dependent on the solvent. In this work, the UV/Vis spectra of the studied compounds were measured in acetonitrile. In order to perform an adequate comparison of the parameters of the different UV/Vis spectra, a line-fitting analysis with Gausssians was performed in a similar manner to that reported earlier by us.[9j] The results obtained are shown in Table 3, and the spectrum of $\mathbf{4}^-$ is shown in Figure 6. Ions $\mathbf{1}^-$ and $\mathbf{3}^-$ give spectra consisting of four absorptions near 210, 280, 340, and 450 nm; the first maximum is one order of magnitude lower than the second. It can be observed that absorptions near 280, 340 and 450 nm are

Table 3. UV/Vis spectra for $\mathbf{1}^-$–$\mathbf{10}^-$ in acetonitrile. λ positions [nm] and ε values [L cm^{-1} mol^{-1}] are reported and were calculated following line-fitting analysis.

	λ (ε)					
$\mathbf{1}^-$	207 (14502)		280 (25943)		340 (2199)	449 (300)
$\mathbf{3}^-$	209 (15028)		283 (24531)		342 (2269)	461 (436)
$\mathbf{4}^-$	222 (3752)		286 (9941)	309 (12687)	360 (1241)	464 (239)
$\mathbf{5}^-$	213 (12343)		282 (10376)	310 (26940)	353 (2553)	465 (340)
$\mathbf{6}^-$			281 (22916)		342 (2528)	460 (560)
$\mathbf{7}^-$			293 (16583)		363 (2178)	492 (504)
$\mathbf{2}^-$	234 (15694)		280 (18672)	314 (5061)	398 (777)	516 (280)
$\mathbf{8}^-$	236 (9911)	270 (5595)	289 (9983)	316 (4779)	376 (930)	500 (290)
$\mathbf{9}^-$	235 (6489)	272 (2415)	291 (6068)	307 (3626)		518 (190)
$\mathbf{10}^-$	234 (12363)	272 (3662)	290 (10887)	324 (4150)	398 (729)	548 (310)

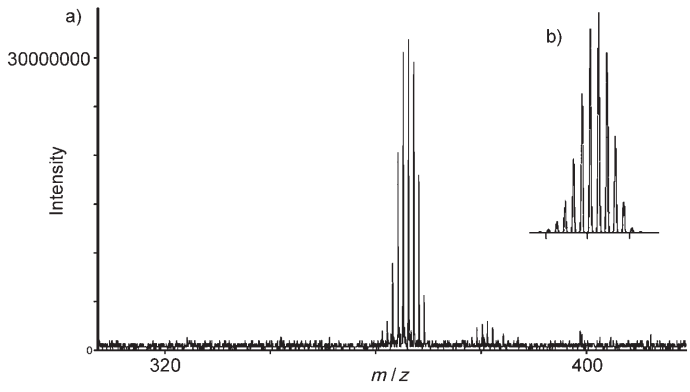

Figure 5. a) Experimental MALDI-TOF mass spectrum obtained for the anion $\mathbf{5}^-$. b) Calculated MALDI-TOF spectrum for $\mathbf{5}^-$.

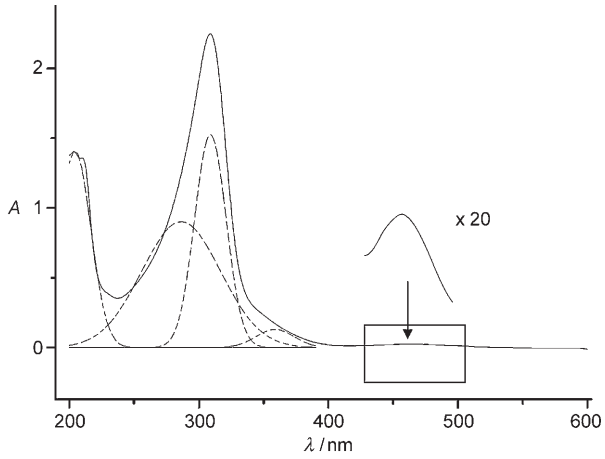

Figure 6. UV/Vis spectrum (solid line) of $\mathbf{4}^-$ and the result of line fitting with Gaussians (dash lines). The expanded section on the right shows the absorption near 445 nm amplified 20 times.

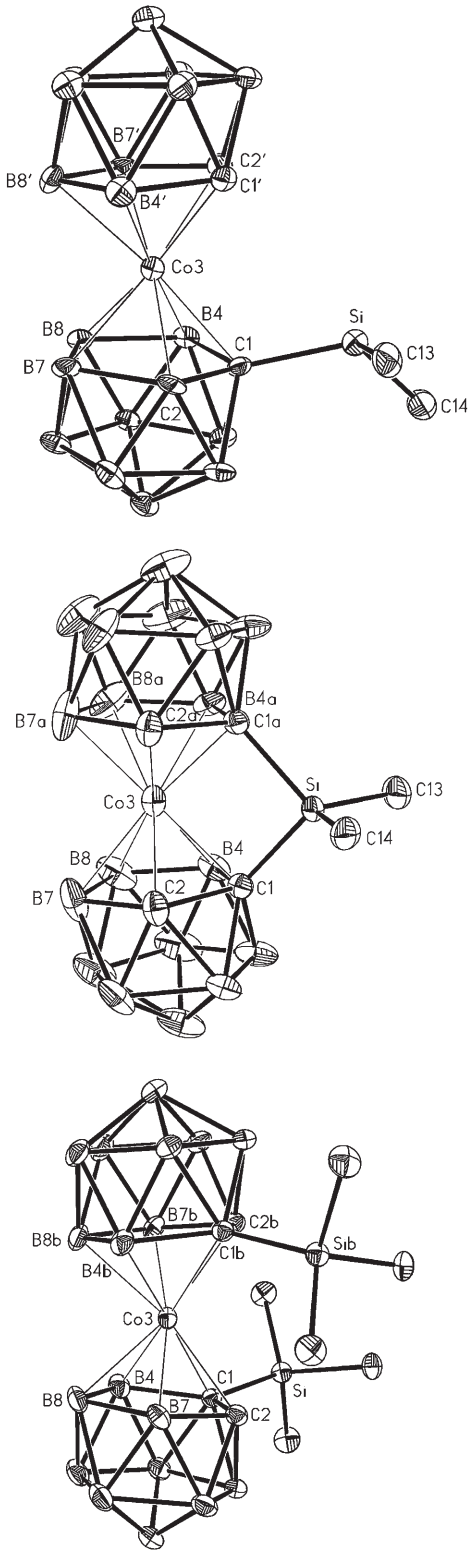

Figure 7. Top: Drawing of the anion of $[NMe_4]$-**3** with 30% thermal displacement ellipsoids. Middle: Drawing of the anion of $[NMe_4]$-**4** with 30% thermal displacement ellipsoids. The "a" refers equivalent position $x, -y+1/2, z$. Bottom: Drawing of the anion of $[NMe_4]$-**7** with 30% thermal displacement ellipsoids. The "b" refers equivalent position $-x+2, y, -z+1/2$. In all cases the hydrogen atoms have been omitted for clarity.

present in all compounds and are attributed to the anion $[3,3\text{-}Co(1,2\text{-}C_2B_9H_{11})_2]^-$, as has already been reported.[9j] The absorption with longest wavelength, near 450 nm, shows a bathochromic shift with respect to $\mathbf{1}^-$ that is larger (about 40 nm) for $\mathbf{7}^-$. This represents a dark red colour in solution or in the solid state. In contrast, the metallacarboranes $\mathbf{1}^-$, $\mathbf{3}^-$, $\mathbf{4}^-$, $\mathbf{5}^-$ and $\mathbf{6}^-$ are orange. It is important to emphasise that the $\mathbf{4}^-$ and $\mathbf{5}^-$ ions show an additional absorbance around 310 nm (Table 3), which could be attributed to the presence of a silyl bridge between the ligands. Compounds prepared from $\mathbf{2}^-$ exhibit a maximum around 230 nm attributed to the benzene moiety.[15c] However, the main differences in the UV/Vis spectra between the precursor and compounds $\mathbf{8}^-$, $\mathbf{9}^-$ and $\mathbf{10}^-$ are due to the presence of an extra signal around 270 nm and a bathochromic shift of 10 nm in the second maximum around 320 nm (Table 3).

X-ray crystallography: Single-crystal X-ray analyses of $[NMe_4]$-**3**, $[NMe_4]$-**4** and $[NMe_4]$-**7** confirmed the expected sandwich structures for the three cobaltabis(dicarbollide) anions. The $\mathbf{3}^-$ ion contains one non-bridging $SiMe_2H$ group, whereas $\mathbf{4}^-$ has a bridging $SiMe_2$ group between the dicarbollide clusters. In $\mathbf{7}^-$, one non-bridging $SiMe_3$ group is bonded to each dicarbollide moiety through the C_c atoms. The structures of $\mathbf{3}^-$, $\mathbf{4}^-$ and $\mathbf{7}^-$ are presented in Figure 7 and selected bond parameters are listed in Tables 4 and 5. It is important to note that for each cobaltabis(dicarbollide) cluster, the presence of the $[NMe_4]^+$ ion is necessary for crystal-

Table 4. Selected bond lengths [Å] and angles [°] for $[NMe_4]$-**3**.

Co3–C1	2.104(6)	Co3–C1′	2.058(6)
Co3–C2	2.056(6)	Co3–C2′	2.048(6)
Co3–B8	2.110(7)	Co3–B8′	2.127(7)
Si–C1	1.907(6)	C1′–C2′	1.608(9
C1–C2	1.627(8)		
Co3-C1-Si	116.8(3)	C1-Co3-C1′	101.2(2)
C1-Co3-C2′	103.6(2)		

Table 5. Selected bond lengths [Å] and angles [°] for $[NMe_4]$-**4**[a] and $[NMe_4]$-**7**[b].

	$[NMe_4]$-**4**	$[NMe_4]$-**7**
Co3–C1	2.0387(16)	2.139(3)
Co3–C2	2.058(2)	2.085(3)
Co3–B4	2.067(2)	2.084(3)
Co3–B7	2.112(3)	2.108(3)
Co3–B8	2.108(3)	2.117(4)
Si–C1	1.8838(16)	1.944(3)
C1–C2	1.668(2)	1.649(4)
Co3-C1-Si	90.47(7)	122.33(15)
C1-Co3-C1a	85.04(9)	
C1-Co3-C1b	132.01(16)	
B8-Co3-B8a	93.71(15)	
B8-Co3-B8b	84.5(2)	

[a] Equivalent positions: a: $x, -y+1/2, z$; [b] Equivalent positions: b: $-x+2, y, -z+1/2$.

lisation of the compounds, since no crystals were obtained with other cations.

The cobaltabis(dicarbollide) anion $\mathbf{3}^-$ has crystallographic C_1 symmetry. The conformation of the dicarbollide clusters is *cisoid*, and the $SiMe_2H$ group is projected between the cluster carbons of the neighbouring $C_2B_9H_{11}^-$ moiety. The conformation can be seen in Figure 7 (top) and by the C1-c-c′-C1′ and C1-c-c′-C2′ torsion angle values of 28.2(4) and −41.3(4)° (c and c′ refer to centres of pentagons C1,C2,B4,B7,B8 and C1′,C2′,B4′,B7′,B8′, respectively). The cobaltabis(dicarbollide) anion of [NMe_4]-**4** assumes σ symmetry with metal and silicon atoms as well as with the methyl carbons lying in the mirror plane (Figure 7, middle). The $SiMe_2$ group is bonded to both clusters through carbon atoms and thus bridge the dicarbollide groups. Owing to the symmetry, the configuration of the dicarbollide ligands is *meso* (the boron cages are in an eclipsed conformation). The anion of [NMe_4]-**7** assumes a two-fold symmetry with the metal lying at the symmetry axis. One $SiMe_3$ group is bonded to a carbon atom of each cage and the groups are oriented so that their disposition in $\mathbf{7}^-$ is *cisoid*, as can be seen in Figure 7 (bottom) and from the C1-c-c[b]-C1[b] dihedral angle of −97.6° (c refers to centre of pentagon C1,C2,B4,B7,B8 and the superscripted b refers equivalent position $-x+2$, y, $-z+1/2$) and the C1-c-c[b]-C2[b] dihedral angle of −26.9°.

A comparison of the structures of $\mathbf{3}^-$, $\mathbf{4}^-$ and $\mathbf{7}^-$ reveals marked differences because of the different silyl groups and bonding modes. Comparing the conformation of $\mathbf{4}^-$ with the ideal cobaltabis(dicarbollide) moiety with parallel coordinating C_2B_3 pentagons, in $\mathbf{4}^-$ the cages are twisted so that the cluster carbons C1 and C1[a] are closer to each other (C1···C1a = 2.755(9) Å, a = x, $-y+1/2$, z). On the opposite side of the coordinating pentagon the distance between the B7 and B7a atoms is increased to 3.10(2) Å. The closing angle on the silicon's side between the two pentagons is 6.91(10)°. In the structures of $\mathbf{3}^-$ and $\mathbf{7}^-$, the influence of the bulky $SiMe_2H$ and $SiMe_3$ groups on the orientation of the coordinating C_2B_3 pentagons is the opposite. The silyl groups repulse the neighbouring pentagons away from each other so that the opening dihedral angle on the silicon atoms' side between the two pentagons are 6.6(2) and 11.16(10)° for $\mathbf{3}^-$ and $\mathbf{7}^-$, respectively.

Theoretical studies related to the formation and conformational structures of compounds: In this section, some aspects related to the formation and characterisation of the anions described above are studied using density functional theory (DFT) calculations.[16] Studies leading to geometric optimisation for ions $\mathbf{1}^-$–$\mathbf{10}^-$ and relative energy calculations were conducted at the B3LYP/6-311G(d,p) level of theory.

Rotational isomers for the metallacarboranes $\mathbf{3}^-$, $\mathbf{6}^-$ and $\mathbf{7}^-$: Three broad conformations for metallacarborane sandwiches exist: *cisoid* (C_{2v}), *gauche* and *transoid* (C_{2h}).[17,18] When relative energy calculations are applied to $\mathbf{1}^-$, it has been reported that the *transoid* conformation is 12.8 kJ mol^{-1} more stable than the *cisoid*.[19] Nevertheless, for the $\mathbf{3}^-$, $\mathbf{6}^-$ and $\mathbf{7}^-$ ions five different conformations are available due to the substitution on the $C_{cluster}$ atoms: two *cisoid*, two *gauche* and one *transoid* rotamers (Figure 8). For $\mathbf{3}^-$, the *gauche* conformation (*gauche*-1) is the more stable than the *cisoid* rotamer (*cisoid*-1) by 2.83 kJ mol^{-1} (Figure 8). In both conformations the Si–H is in proximity to C_c–H, facilitating a dihydrogen interaction. In fact, the *cisoid*-1 corresponds to the rotamer found in the crystal structure. However, in the C_c-monosubstituted $\mathbf{6}^-$ ion, the *gauche* conformation (*gauche*-2) is the more stable, being 3.03 and 4.20 kJ mol^{-1} more stable than the *transoid* and *cisoid*-2 rotamers, respectively (Figure 8). The difference on the relative energies between rotamers of $\mathbf{3}^-$ and $\mathbf{6}^-$ is most probably due to the dihydrogen interactions in the case of $\mathbf{3}^-$. In addition, $\mathbf{7}^-$, like other C_c-disubstituted derivatives of cobaltabis(dicarbollide),[11] revealed that the synthesised geometrical isomer shows racemic substitution according to the X-ray diffraction study, and the dicarbollide ligands are rotated with respect to each other along the axis passing through B10 and B10′. Using the B8-Co3-B10-B8 dihedral angle "q"[19] as a parameter for the dicarbollide ligands rotation, a rotational energy path profile was calculated by using optimised structures of $\mathbf{7}^-$. Three minima for q = 38.1° (*cisoid*-2), 122.3° (*gauche*-2) and 197.4°

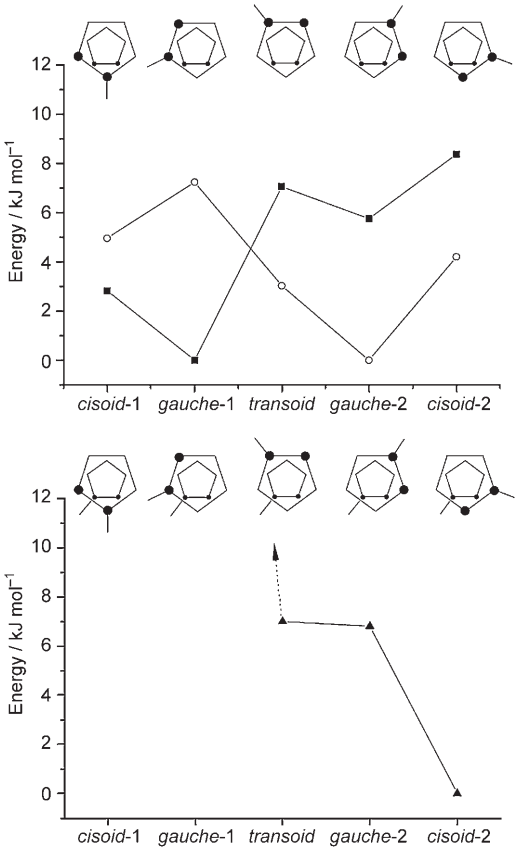

Figure 8. Calculated relative energies and conformational isomers for compounds $\mathbf{3}^-$ (■), $\mathbf{6}^-$ (○) and $\mathbf{7}^-$ (▲).

(*transoid*) were obtained with relative energies 0, 6.8 and 7.0 kJ mol^{-1}, respectively (Figure 8). The minimum energy conformer found with $q = 38.1°$ corresponds to the *cisoid* rotamer and agrees well with what was found in the crystal structure. However, for **7**$^-$, the relative energies of *cisoid*-1 and *gauche*-1 were not possible to calculate due to the steric hindrance.

Proposed mechanism for the formation of compounds **4**$^-$ *and* **8**$^-$*—comparison of the theoretical and experimental results*: In the course of this research two questions have arisen: 1) why is it possible to get the C_c-monosubstitution on **1**$^-$ by using one equivalent of *n*BuLi and Me_2SiHCl to give **3**$^-$, whereas its homologous derivative from **2**$^-$ was never detected; and 2) why is compound **4**$^-$ obtained as a byproduct in the synthesis of **3**$^-$, while its homologue **8**$^-$ is the main product in a similar reaction from **2**$^-$?. These questions may both be answered taking into account an "intramolecular reaction" that leads to the formation of the bridging μ-$SiMe_2$ group. A possible pathway that explains this intramolecular reaction is shown in Scheme 5. After the formation of the monolithium salt of **1**$^-$ or **2**$^-$, a C_c-monosubstituted compound with a $-SiMe_2H$ group is generated. The geometrical disposition of one acidic C_c–H proton and the hydride of the Si–H function favours the elimination of H_2 with the formation of the second C_c–Si bond. Theoretical calculations were carried out to corroborate this mechanism in the case of **8**$^-$ from **2**$^-$. In the latter, the rotation around the metallic centre is hindered by the presence of the phenyl group bonded both to B8 and B8′, which provides a stable eclipsed *cisoid* configuration (Scheme 5). Thus, the geometry of a hypothetical C_c-monosubstituted intermediate derivative of **2**$^-$ with a $SiMe_2H$ group, which has never been isolated (Scheme 5), was optimised. A natural population analysis (NPA) was carried out to determine the charges of the hydrogen atoms that may be involved in the intramolecular reaction. The charge on Si–H is −0.194 (more negative that the Si–H in $SiMe_2HCl$, which is −0.185), and the charge of the hydrogen in C_c–H is +0.306 (more acidic than **2**$^-$, which is +0.265). The opposite charges should then favour the interaction between both hydrogen atoms to give the C_c-disubstituted ion **8**$^-$ (Scheme 5). Additionally, a transition state for the formation of **8**$^-$ was found by using the synchronous transit-guided quasi-newton (STQN) method. Figure 9 shows the optimised structure of this transition state. In addition, using the equation $\Delta G(T) = \Delta H(T) - T\Delta S(T)$, the enthalpy for the intramolecular reaction proposed in this mechanism has also been calculated and is endothermic at −78 °C (195 K), ($\Delta_r H^{195} = +37.2$ kJ mol^{-1}) and not spontaneous ($\Delta_r G^{195} = +13.8$ kJ mol^{-1}). Plotting $\Delta_r G$ versus the temperature (T), it is observed that at $T = 32$ °C (305 K) the Gibbs free energy becomes negative as is shown in Figure 10. The evolution of $\Delta_r G$ to negative values is a consequence of the entropic terminus in the state equation. It may be concluded that due to the required *cisoid* conformation for this reaction to occur, in the case of **2**$^-$, the intramolecular reaction leading to **8**$^-$ is favoured; in contrast, the corresponding monosubstituted compound from **2**$^-$, equivalent to **3**$^-$, is never observed.

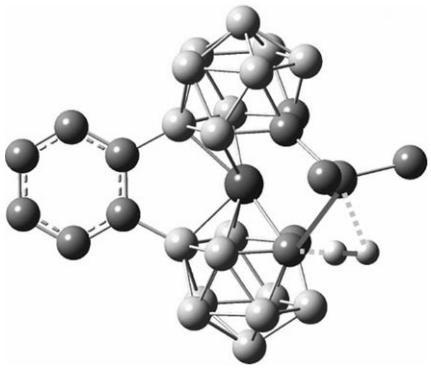

Figure 9. The transition state found for the intramolecular reaction to obtain **8**$^-$. This minimum has a single imaginary frequency corresponding to the vibrational modes of the hydrogen involved in the reaction. Dash lines represent the cleaved bonds and solid lines represent the new bonds.

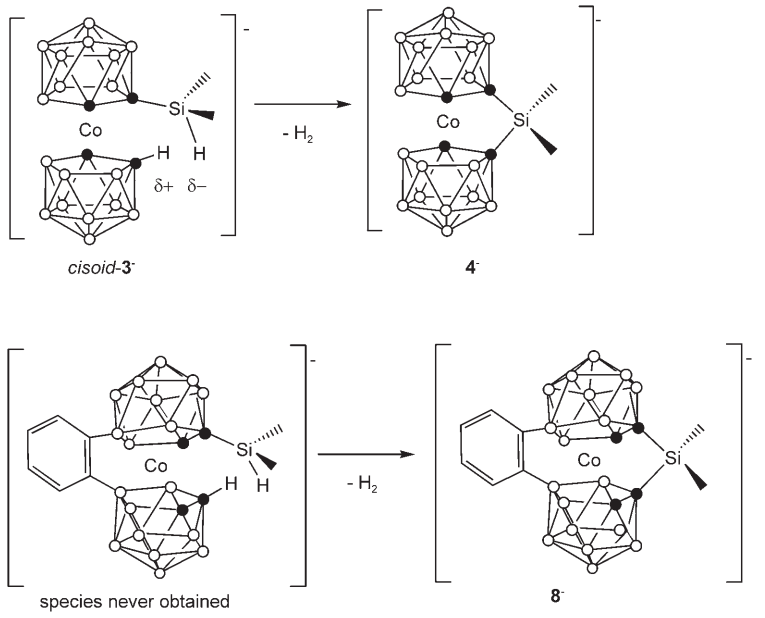

Scheme 5. Suggested pathway for the intramolecular reaction that causes a bridge between both dicarbollide clusters in ions **4**$^-$ and **8**$^-$.

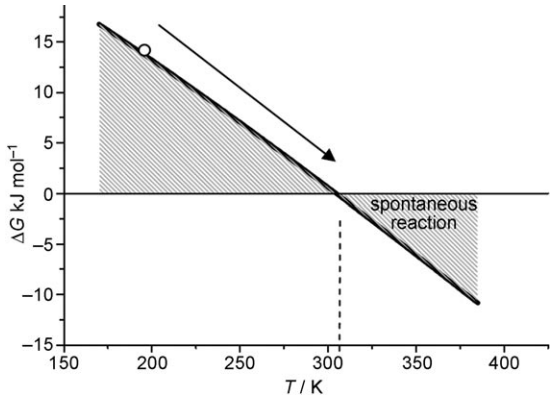

Figure 10. Gibbs free-energy temperature dependence calculated for the intramolecular reaction: $\Delta G(T) = \Delta H(T) - T\Delta S(T)$.

Theoretical calculations of the relative energy for the optimised conformation in $\mathbf{3}^-$ indicated that the *cisoid*-1 conformation observed in the crystal structure, in which the Si–H group is closest to the C_c–H, is 10.96 kJ mol^{-1} more stable than the same rotamer, but with the Si–H rotated and farthest from the C_c–H. The stability of this structure is then attributed to the existence of two intramolecular dihydrogen interactions, C_c–H···H–Si, 2.44 and 2.16 Å, according to the DFT calculations. These match well with those found in the crystal structure, 2.409 and 2.212 Å. This provides an explanation to the first question about the formation of $\mathbf{3}^-$. In addition, experimental results have shown that the temperature is critical in the reaction leading to $\mathbf{3}^-$ and $\mathbf{4}^-$. By keeping the reagents and solvents at −40 °C or higher, only $\mathbf{4}^-$ was formed, whereas at −78 °C a mixture of $\mathbf{3}^-$ and $\mathbf{4}^-$ is obtained (see Scheme 1). Therefore, we hypothesise that the formation of $\mathbf{4}^-$ is clearly dependent on the temperature, and the activation barrier of this process is favoured at higher temperatures. Increasing the reaction temperature favours the intramolecular dihydrogen contacts (Scheme 5), which is assumed to precede the formation of H_2 from the reaction of one positive and one negative hydrogen atom, corroborating the mechanism proposed to explain the intramolecular process.[20] Consequently, $\mathbf{3}^-$ may be obtained only if very low reaction temperatures are used.

Geometrical isomers for compounds $\boldsymbol{4}^-$, $\boldsymbol{5}^-$ *and* $\boldsymbol{9}^-$: The ions $\mathbf{4}^-$, $\mathbf{5}^-$ and $\mathbf{9}^-$ may form structural isomers, which are dependent on the reaction temperature. Complex $\mathbf{4}^-$ has three geometrical isomers, two enantiomers and one diastereomer, the structures of which are the racemic mixture *rac*-$\mathbf{4}^-$ and the meso isomer *meso*-$\mathbf{4}^-$, respectively (Figure 11). In the *rac*-$\mathbf{4}^-$ isomers, both methyl groups bonded to the Si atom are equivalent. However, the *meso*-$\mathbf{4}^-$ isomer has eclipsed C_c atoms and non-equivalent methyl groups because one CH_3 faces the two non-substituted cluster carbon atoms, whereas the other does not. Theoretical calculations have shown that the *rac*-$\mathbf{4}^-$ form is 12.7 kJ mol^{-1} more stable than *meso*-$\mathbf{4}^-$. Therefore, and if only thermodynamic conditions are taken into account, it could be hypothesised that when

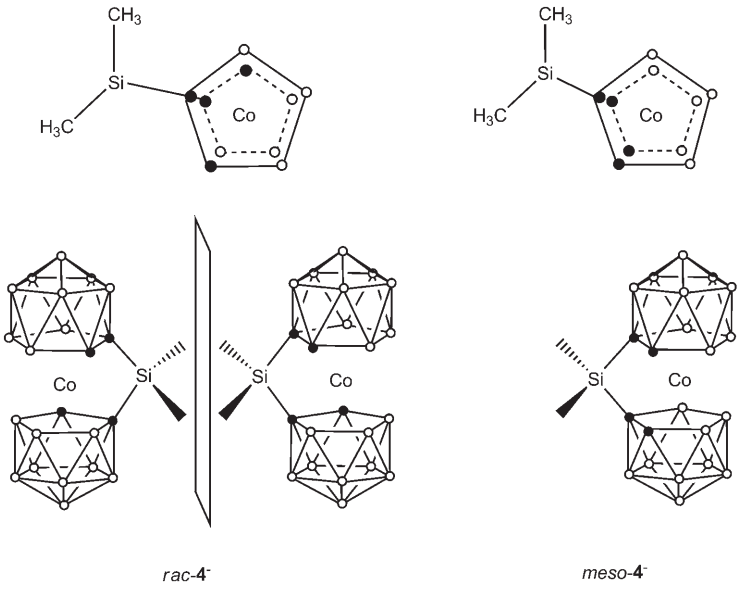

Figure 11. Geometrical isomers of compound $\mathbf{4}^-$. Top: Plane projections of the pentagonal faces. Bottom: *rac*-$\mathbf{4}^-$ sketching of *d* and *l* enantiomers and isomer *meso*-$\mathbf{4}^-$.

$\mathbf{4}^-$ was prepared at −78 °C, the resonances observed in the $^{11}B\{^1H\}$ NMR spectrum were mostly due to the *rac*-$\mathbf{4}^-$, and other signals of lower intensity were assigned to the less stable isomer, *meso*-$\mathbf{4}^-$ (Figure 12 top). This was confirmed when $\mathbf{4}^-$ was synthesised at 0 °C and −40 °C, at which temperatures the *meso*-$\mathbf{4}^-$ isomer is more abundant according to the ^{11}B NMR spectrum (Figure 12 bottom). To corroborate

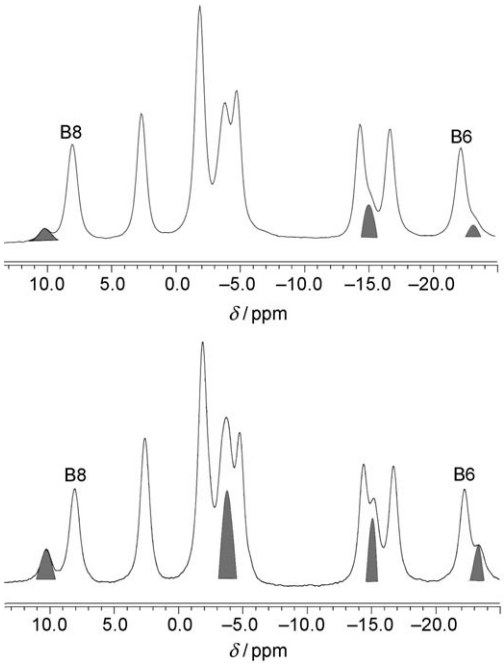

Figure 12. $^{11}B\{^1H\}$ NMR spectra of the anion $\mathbf{4}^-$. The shaded areas are attributed to the boron atoms of *meso*-$\mathbf{4}^-$. Top: $\mathbf{4}^-$ synthesised at −78 °C. Bottom: $\mathbf{4}^-$ synthesised at $T > -40$ °C.

this interpretation, the $^{11}B\{^1H\}$ NMR absolute shielding of *meso*-**4**$^-$ and *rac*-**4**$^-$ were calculated at the GIAO/B3LYP/6-31++G(d) level of theory.[21] The $^{11}B\{^1H\}$ NMR theoretical chemical shifts for **4**$^-$ exhibit a resonance assigned to B8 atoms and shifted 4.5 ppm to lower field in *meso*-**4**$^-$ than in the *rac*-**4**$^-$. In addition, calculations indicate that B6 atoms in the *meso*-**4**$^-$ form are shifted 2 ppm to higher field than the isomer *rac*-**4**$^-$. The experimental values for B8 and B6 for *meso*-**4**$^-$ are 10.34 and −23.36 ppm, and for *rac*-**4**$^-$ they are 8.07 and −22.11 ppm, respectively. Although the theoretical values do not fit exactly with the experimental values, they are indicative of the patterns' tendency. This confirms that at −78 °C the *rac*-**4**$^-$ enantiomers are mostly obtained, whereas at higher temperatures the *meso*-**4**$^-$ can be also isolated. Specifically, the crystal structure of $[NMe_4]$-**4** (Figure 7, middle) corresponds to the *meso*-**4**$^-$ isomer and was obtained from the crystallisation of a reaction carried out at −40 °C.

Four different geometrical isomers could be expected for **5**$^-$: a pair of enantiomers and two diastereomers, which should correspond to the racemic mixture (or *rac* isomers) and two *meso* isomers. For the latter, we have used the notation M and m to identify the major and minor diastereomers, respectively (Figure 13). Theoretical calculations indicate that the *rac*-**5**$^-$ form is 10.5 and 15.4 kJ mol^{-1} more stable than isomers *meso*(M)-**5**$^-$ and *meso*(m)-**5**$^-$, respectively. The stability of *meso*(M)-**5**$^-$ over *meso*(m)-**5**$^-$ could be anticipated by considering the possible coulombic interactions shown in the plane projection (Figure 13). When **5**$^-$ was prepared at −78 °C, the ^1H NMR spectrum shows only one resonance due to the Si–H proton and attributed to the racemic mixture or *rac*-**5**$^-$ (Figure 14a). Nevertheless, when **5**$^-$ was prepared at higher temperatures (−40 °C), a mixture of three compounds appeared in the ^1H NMR spectrum and were assigned to the Si–H and SiMe protons. Resonances

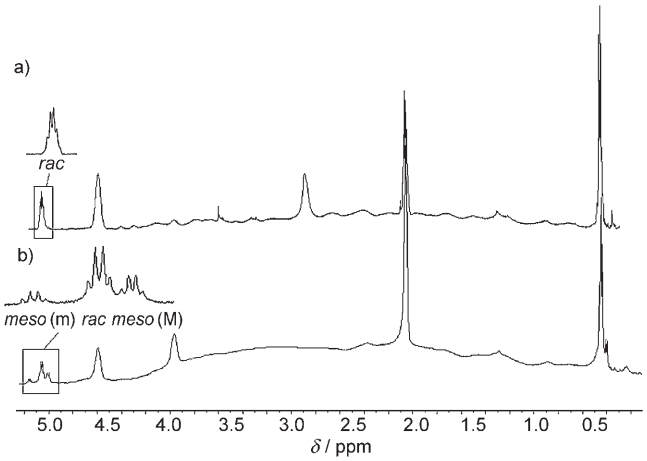

Figure 14. ^1H NMR spectra of Cs-**5** synthesised at different temperatures: a) −78 °C and b) > −40 °C.

were assigned according to the relative energies calculated for isomers, and an integration of signals indicated the formation of *rac*-**5**$^-$, *meso*(M)-**5**$^-$ and *meso*(m)-**5**$^-$ in the percentage of 65, 22 and 13, respectively (Figure 14b).

Finally, compound **9**$^-$ may form two different diastereomers or *meso* isomers, denoted as *meso*(M)-**9**$^-$ and *meso*(m)**9**$^-$ (Figure 15), because the impossibility of rotating the ligands prevents the formation of the *rac* isomer. Theoretical calculations indicate again that *meso*(M)-**9**$^-$ is just 5.70 kJ mol^{-1} more stable than isomer *meso*(m)**9**$^-$. Consequently, when **9**$^-$ was prepared, even at very low temperatures (−78 °C), a mixture of both isomers was observed according to the ^1H NMR spectrum (see Experimental Section).

Therefore, we can confirm that for these metallacarboranes, the racemic mixture (or *rac* form) is the most stable

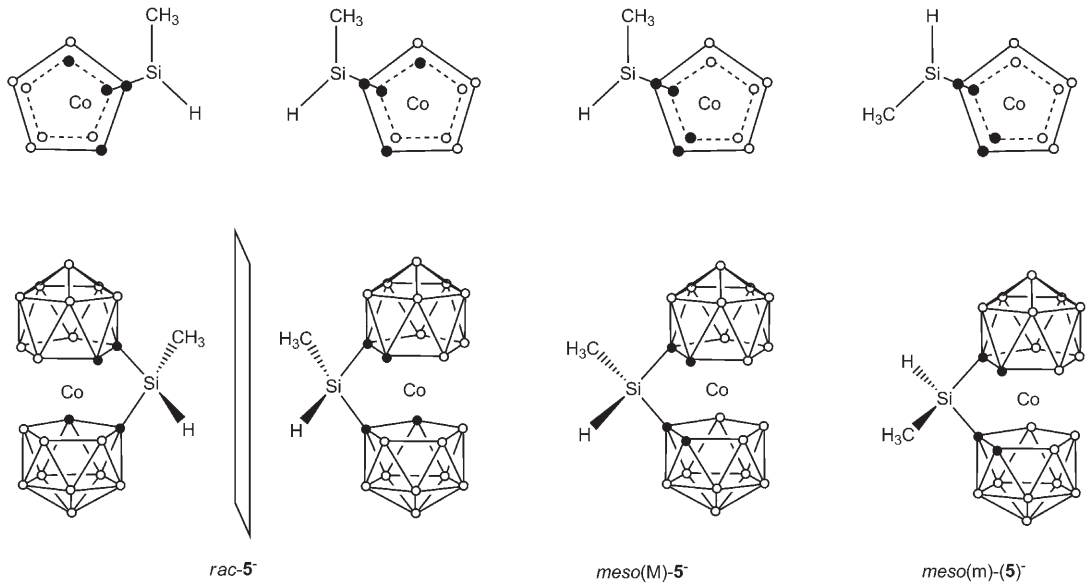

Figure 13. The *rac*-**5**$^-$ and *meso*-**5**$^-$ structures for **5**$^-$.

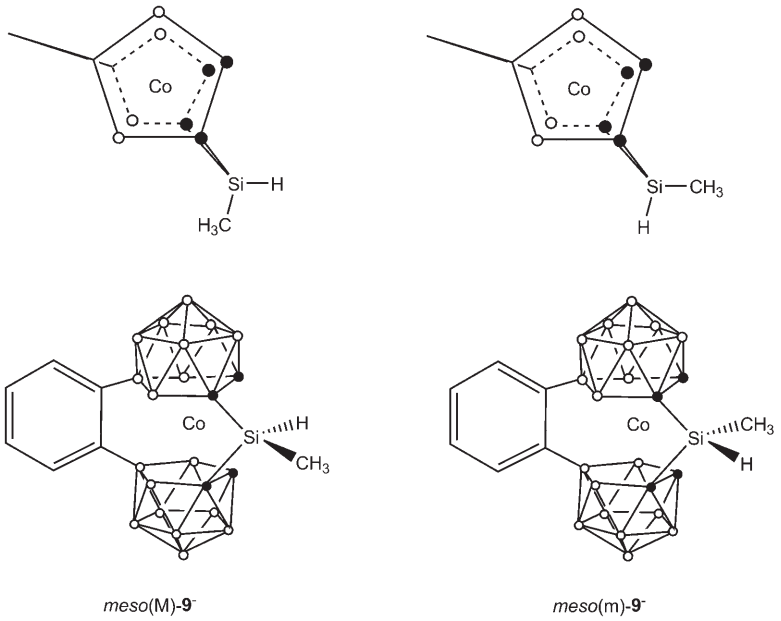

Figure 15. The *meso* isomers for anion $\mathbf{9}^-$.

and the main reaction product, followed by the *meso* isomer with the CH_3 groups projected on the clusters B–H, *meso*(M). Finally the least stable would be the *meso* isomer with the $-CH_3$ group projected on the C_c–H, *meso*(m).

Conclusion

The first C_c-mono and C_c-disubstituted cobaltabis(dicarbollide) derivatives containing different organosilane functions have been successfully prepared by the direct reaction of the mono or dilithium salts of starting anions $\mathbf{1}^-$ and $\mathbf{2}^-$ with the appropriate chlorosilanes and under careful monitoring of the temperature. The reaction temperature was a key factor in the direct reaction to major isomers, since at very low temperatures (−78 °C) C_c-monosubstituted species and high isomeric purity were obtained, whereas increasing the temperature (−40 °C or 0 °C) led to C_c-disubstituted anions and structural isomeric mixtures. The ion $\mathbf{3}^-$ represents the first example of a C_c-monosubstituted cobaltabis(dicarbollide) derivative that has been fully characterised by X-ray diffraction analysis. Compounds $\mathbf{4}^-$ and $\mathbf{8}^-$, containing a bridging (-μ-$SiMe_2$) between both dicarbollide ligands, were obtained unexpectedly from the reaction of the respective monolithium salt of $\mathbf{1}^-$ or $\mathbf{2}^-$ with Me_2SiHCl at low temperatures. A hypothetical mechanism has been proposed to explain the formation of these compounds through an intramolecular interaction and has been supported by theoretical calculations compared with experimental results. Density functional theory (DFT) at the B3LYP/6-311G(d,p) level was applied to optimise the geometries of ions $\mathbf{1}^-$–$\mathbf{10}^-$ and calculate their relative energies. The theoretical studies perfectly agree with the experimental results, indicating that *rac* isomers are more stable than *meso* isomers. Some of the metallacarboranes $\mathbf{3}^-$, $\mathbf{5}^-$ and $\mathbf{9}^-$ functionalised with −SiH have actually been used as hydrosilylating agents to be attached to the periphery of dendrimeric structures by the hydrosilylation of alkenes.

Experimental Section

General considerations: Elemental analyses were performed by using a Carlo Erba EA1108 microanalyser. FTIR spectra were recorded with KBr pellets on a Shimadzu FTIR-8300 spectrophotometer. UV/Vis spectroscopy was carried out with a Shimadzu UV/Vis 1700 spectrophotometer with 1 cm cuvettes. The concentration of the complexes was 1×10^{-4} M. UV/Vis spectra were measured using the following procedure: stock solutions of the compounds were prepared by making a solution of several milligrams of the solid compound in 5 mL of acetonitrile (HPLC grade, Sigma-Aldrich). After this, a sample of this stock solution was diluted to a concentration of 10^{-4} M. The matrix-assisted laser desorption ionisation time-of-flight mass spectra (MALDI-TOF-MS) were recorded in the negative ion mode with a Bruker Biflex MALDI-TOF instrument (N_2 laser; λ_{exc} 337 nm (0.5 ns pulses); voltage ion source 20.00 kV (Uis1) and 17.50 kV (Uis2)). ^{1}H and ^{1}H{^{11}B} NMR (300.13 MHz), ^{13}C{^{1}H} NMR (75.47 MHz), ^{11}B and ^{11}B{^{1}H} NMR (96.29 MHz), and ^{29}Si{^{1}H} (59.62 MHz) spectra were recorded at room temperature on a Bruker ARX 300 instrument equipped with the appropriate decoupling accessories. All NMR measurements were performed in [D_6]acetone at 22 °C. Chemical shift data for ^{1}H, ^{1}H{^{11}B}, ^{13}C{^{1}H}and ^{29}Si{^{1}H} NMR spectra are referenced to $SiMe_4$; those for ^{11}B{^{1}H} and ^{11}B NMR spectra are referenced to external $BF_3{\cdot}OEt_2$. Chemical shifts are reported in ppm, followed by a description of the multiplet (e.g. d = doublet), its relative intensity and observed coupling constants (in Hz). Unless otherwise noted, all manipulations were carried out in a nitrogen atmosphere using standard vacuum line techniques. Solvents were purified by distillation from appropriate drying agents before use. 1,2-Dimethoxyethane (DME) was distilled from sodium/benzophenone prior to use. The metallacarboranes Cs[3,3′-Co(1,2-$C_2B_9H_{11})_2$] (Cs-**1**) and Cs[8,8′-μ-(1″,2″-C_6H_4)-3,3′-Co(1,2-$C_2B_9H_{10})_2$], (Cs-**2**) were commercially obtained from KATCHEM. *n*-Butyllitium (1.6 M in hexane) was purchased from Alfa Aesar; $MeSiHCl_2$ and Me_2SiHCl were obtained from Aldrich; Me_2SiCl_2 and Me_3SiCl were purchased from FluoroChem, and were used as received. The [NMe_4]Cl was purchased from Panreac, and CsCl and [$PMe(Ph)_3$]Br were received from Fluka.

Synthesis of [NMe_4][1-$SiMe_2$H-3,3′-Co(1,2-$C_2B_9H_{10}$)(1′,2′-$C_2B_9H_{11}$)] ([NMe_4]-3): *n*BuLi (0.50 mL, 0.79 mmol) was added dropwise to a Schlenk flask containing a stirred solution of Cs-**1** (360 mg, 0.79 mmol) in DME (12 mL) at −78 °C. The low-temperature bath was removed and the purple suspension was stirred for 45 min. The suspension was then cooled to −78 °C and Me_2SiHCl (0.10 mL, 0.88 mmol) was added dropwise. The suspension was stirred at room temperature for 1 h to give an orange solution and a white solid. The solid was filtered off and the solution evaporated to dryness. The residue was dissolved in MeOH (0.5 mL) and an aqueous solution of [NMe_4]Cl (50 mg, 7 mL) was added dropwise to give an orange solid. The solid was washed with H_2O (2×15 mL) and hexane (2×15 mL). The resultant solid was purified from a solution of CH_2Cl_2 to afford [NMe_4]-**3** (yield: 40 mg, 11 %). Alternatively, the addi-

tion of an aqueous solution of CsCl to the residue dissolved in MeOH (0.5 mL) gave an orange solid. The solid was washed with H_2O (2× 15 mL) and hexane (2×15 mL) and subsequently purified several times using a mixture of Et_2O/CH_2Cl_2 (1:1) to afford Cs-**3** (yield: 16 mg, 4%). $^1H\{^{11}B\}$ NMR: $\delta=4.31$ (sept, $^3J(H,H)=3.4$, 1H; Si-*H*), 3.85 (brs, 1H; $C_{cluster}$-*H*), 3.69 (brs, 2H; $C_{cluster}$-*H*), 3.45 (s, 12H; N-CH_3), 0.29 ppm (d, $^3J(H,H)=3.4$, 6H; Si-CH_3); $^{13}C\{^1H\}$ NMR: $\delta=57.00$ (N-CH_3), 55.57 (C_c-H), 51.65 (C_c-H), 49.26 (C_c-Si), −1.34 ppm (Si-CH_3); ^{11}B NMR: $\delta=9.10$ (d, $^1J(H,B)=163$, 1B; B8′), 7.29 (d, $^1J(H,B)=146$, 1B; B8), 3.56 (d, $^1J(H,B)=121$, 1B; B10′), 2.50 (d, $^1J(H,B)=123$, 1B; B10), −1.70 (d, $^1J(H,B)=143$, 1B; B12′), −4.65 (d, 4B; B4,4′,7′,9′), −5.00 (d, 3B; B4,7,9,12), −14.25 (d, $^1J(H,B)=159$, 2B; B5′,11′), −16.79 (d, $^1J(H,B)=156$, 2B; B5,11), −21.15 (d, $^1J(H,B)=106$, 1B; B6′), −22.26 ppm (d, $^1J(H,B)=111$, 1B; B6); $^{29}Si\{^1H\}$ NMR: $\delta=-8.28$ ppm; IR: $\tilde{\nu}=3040$ (C_c–H), 2557 (B–H), 2160 (Si–H), 1481 (C–N), 1254 cm^{-1} (Si–CH_3); MALDI-TOF-MS: *m/z* calcd for $[M-NMe_4]^-$: 382.3; found: 382.2; elemental analysis calcd (%) for $C_{10}H_{40}B_{18}CoNSi$: C 26.34, H 8.84, N 3.07; found: C 26.55, H 8.85, N 3.12.

Synthesis of Cs[1,1′-μ-SiMe$_2$-3,3′-Co(1,2-C$_2$B$_9$H$_{10}$)$_2$] (Cs-4)

Method A: The procedure was similar to that used to prepare Cs-**3**, with Cs-**1** (105 mg, 0.23 mmol) in DME (10 mL) at −40 °C, *n*BuLi (0.15 mL, 0.24 mmol) and Me_2SiHCl (35 μL, 0.31 mmol). After addition of Me_2SiHCl, the suspension was stirred at room temperature for 3 h. The suspension was filtered and the solution evaporated to dryness giving a brown-orange residue of [Li(dme)$_2$]-**4**, according to the ^1H NMR spectrum. At this point, different cations were used to isolate the **4**$^-$ ion. [Li(dme)$_2$]-**4** (100 mg, 0.18 mmol) was dissolved in MeOH (0.3 mL) and an aqueous solution of CsCl was added dropwise to give an orange solid. The solid was washed with H_2O (2×15 mL) and hexane (2×15 mL) to obtain Cs-**4** (yield: 73 mg, 62%). Alternatively, the addition of an aqueous solution of $[NMe_4]Cl$ to the orange residue of [Li(dme)$_2$]-**4** (100 mg, 0.18 mmol) dissolved in MeOH led to[NMe_4]-**4** (yield: 47 mg, 45%). Orange crystals suitable for an X-ray diffraction study were grown by slow evaporation of a solution of [NMe_4]-**4** in acetoneat room temperature. Furthermore, [PMe(Ph)$_3$]-**4** (yield: 83 mg, 70%) was also isolated from the addition of a methanolic solution of [PMe(Ph)$_3$]Br to the orange residue of [Li(dme)$_2$]-**4** dissolved in MeOH.

Method B: The procedure was similar to that used to prepare Cs-**3**, with Cs-**1** (360 mg, 0.79 mmol) in DME (12 mL) at −78 °C, *n*BuLi (1 mL, 1.60 mmol) and Me_2SiCl_2 (0.20 mL, 1.66 mmol). After addition of Me_2SiCl_2, the suspension was stirred at room temperature for 3 h. Then, the suspension was filtered and the solution evaporated to dryness giving a brown-orange residue of [Li(dme)$_2$]-**4** (426 mg). [Li(dme)$_2$]-**4** (100 mg, 0.18 mmol) was dissolved in MeOH (0.6 mL) and the dropwise addition of an aqueous solution of CsCl gave an orange solid. The solid was washed with H_2O (2×15 mL) and hexane (2×15 mL) to afford Cs-**4** (yield: 69 mg, 71%). ^1H NMR: $\delta=4.50$ (brs, 2H; C_c-*H*), 0.31 ppm (s, 6H, Si-CH_3); $^{13}C\{^1H\}$ NMR: $\delta=55.59$ (C_c-H), 41.68 (C_c-Si), −4.12 ppm (Si-CH_3); ^{11}B NMR: $\delta=8.07$ (d, $^1J(H,B)=142$ Hz; 2B), 2.70 (d, $^1J(H,B)=141$ Hz; 2B), −1.83 (d, $^1J(H,B)=150$ Hz; 4B), −3.78 (d, $^1J(H,B)=138$ Hz; 2B), −4.70 (d, $^1J(H,B)=128$ Hz, 2B), −14.29 (d, $^1J(H,B)=160$ Hz, 2B), −15.61 (d, $^1J(H,B)=157$ Hz, 2B), −22.11 ppm (d, $^1J(H,B)=165$ Hz, 2B); $^{29}Si\{^1H\}$ NMR: $\delta=13.98$ ppm; IR: $\tilde{\nu}=3070$ (C_c–H), 2554 (B–H), 1256 cm^{-1} (Si–CH_3); MALDI-TOF-MS: *m/z* calcd for $[M-Cs]^-$: 380.33; found: 380.34; elemental analysis calcd (%) for $C_6H_{26}B_{18}CoCsSi$: C 14.05, H 5.11; found: C 13.75, H 4.84.

Synthesis of Cs[1,1′-μ-SiMeH-3,3′-Co(1,2-C$_2$B$_9$H$_{10}$)$_2$] (Cs-5): The procedure was similar to that used to prepare Cs-**4**, with Cs-**1** (500 mg, 1.10 mmol) in DME (14 mL) at −78 °C, *n*BuLi (1.40 mL, 2.24 mmol) and $MeSiHCl_2$ (0.30 mL, 2.82 mmol). After addition of $MeSiHCl_2$, the suspension was stirred at room temperature for 6 h. The suspension was filtered and the solution evaporated to dryness. The residue was dissolved in MeOH (0.30 mL) and a solution of CsCl in water was added dropwise to give an orange solid. The solid was washed with H_2O (2×15 mL) and hexane (2×15 mL) to afford of Cs-**5** (yield: 417 mg, 76%). ^1H NMR: $\delta=5.06$ (q, $^3J(H,H)=3.4$ Hz, 1H; Si-*H*), 4.59 (brs, 2H; C_c-*H*), 0.44 ppm (d, $^3J(H,H)=3.4$ Hz, 3H,; Si-CH_3); $^{13}C\{^1H\}$ NMR: $\delta=55.86$ (C_c-H), 53.89 (C_c-H), 36.67 (C_c-Si), −6.76 ppm (Si-CH_3); ^{11}B NMR: $\delta=8.20$ (d, $^1J(H,B)=140$ Hz, 2B), 2.80 (d, $^1J(H,B)=141$ Hz, 2B), −1.72 (d, $^1J(H,B)=143$ Hz, 4B), −3.20 (d, $^1J(H,B)=131$ Hz, 1B), −4.63 (d, $^1J(H,B)=131$ Hz, 3B), −13.95 (d, $^1J(H,B)=162$ Hz, 1B), −14.37 (d, $^1J(H,B)=162$ Hz, 1B), −16.13 (d, $^1J(H,B)=162$ Hz, 1B), −16.74 (d, $^1J(H,B)=162$ Hz, 1B), −20.23 (d, $^1J(H,B)=108$–, 1B), −22.24 ppm (d, $^1J(H,B)=105$ Hz, 1B); $^{29}Si\{^1H\}$ NMR: $\delta=2.94$ ppm; IR: $\tilde{\nu}=3063$ (C_c–H), 2554 (B–H), 2160 (Si–H), 1257 cm^{-1} (Si–CH_3); MALDI-TOF-MS: *m/z* calcd for $[M-Cs]^-$: 366.33; found: 366.2; elemental analysis calcd (%) for $C_5H_{24}B_{18}CoCsSi$: C 12.04, H 4.85; found: C 12.62, H 4.95.

Synthesis of Cs[1-SiMe$_3$-3,3′-Co(1,2-C$_2$B$_9$H$_{10}$)(1′,2′-C$_2$B$_9$H$_{11}$)] (Cs-6): The procedure was similar to that used to prepare Cs-**3**, with Cs-**1** (205 mg, 0.45 mmol) in DME (8 mL) at −78 °C, *n*BuLi (0.30 mL, 0.48 mmol) and Me_3SiCl (0.10 mL, 0.77 mmol). After addition of Me_3SiCl, the suspension was stirred at room temperature for 5 h to give a red solution and a white solid. The solid was filtered off and the solution evaporated to dryness. The residue was dissolved in MeOH (0.20 mL) and a solution of [NMe_4]Cl (50 mg) in water (7 mL) was added dropwise to give a red solid. The solid was washed with H_2O (2×10 mL) and hexane (2× 10 mL). The resultant solid was purified from CH_2Cl_2 to afford [NMe_4]-**6** (yield: 70 mg, 33%). Alternatively, the addition of an aqueous solution of CsCl to the residue dissolved in MeOH (0.5 mL) gave an orange solid. The solid was washed with H_2O (2×15 mL) and hexane (2×15 mL) and subsequently purified several times using a mixture of Et_2O/CH_2Cl_2 (1:1) to afford Cs-**6** (yield: 36 mg, 15%). $^1H\{^{11}B\}$ NMR: $\delta=4.02$ (brs, 1H; C_c-*H*), 3.83 (brs, 1H; C_c-*H*), 3.72 (brs, 1H; C_c-*H*), 0.28 ppm (s, 9H; Si-CH_3); $^{13}C\{^1H\}$ NMR: $\delta=59.04$ (C_c-H), 52.84 (C_c-H), 50.54 (C_c-H), 48.66 (C_c-Si), 3.08 ppm (Si-CH_3); ^{11}B NMR: $\delta=8.20$ (d, $^1J(H,B)=181$ Hz, 1B), 6.10 (d, $^1J(H,B)=180$ Hz, 1B), 3.53 (d, $^1J(H,B)=155$ Hz, 1B), 1.19 (d, $^1J(H,B)=143$ Hz, 1B), −1.95 (d, $^1J(H,B)=142$ Hz, 1B), −4.04 (1B), −5.60 (2B), −6.32 (2B), −7.32 (2B), −14.26 (d, $^1J(H,B)=143$ Hz, 1B), −15.15 (d, $^1J(H,B)=154$ Hz, 1B), −17.58 (d, $^1J(H,B)=154$ Hz, 1B), −18.40 (d, $^1J(H,B)=144$ Hz, 1B), −21.40 (d, $^1J(H,B)=165$ Hz, 1B), −23.06 ppm (d, $^1J(H,B)=161$ Hz, 1B); $^{29}Si\{^1H\}$ NMR: $\delta=10.74$ ppm; IR: $\tilde{\nu}=3090$ (C_c–H), 3038 (C_c–H), 2562 (B–H), 1259 cm^{-1} (Si–CH_3); MALDI-TOF-MS: *m/z* calcd for $[M-Cs]^-$: 396.37; found: [*M*-Cs]$^-$ 396.3; elemental analysis calcd (%) for $C_7H_{30}B_{18}CoCsSi$: C 15.89, H 5.72; found: C 15.47, H 5.69.

Synthesis of Cs[1,1′-(SiMe$_3$)$_2$-3,3′-Co(1,2-C$_2$B$_9$H$_{10}$)$_2$] (Cs-7): *n*BuLi (0.60 mL, 0.96 mmol) was added dropwise to a Schlenk flask containing a stirred solution of Cs-**1** (214 mg, 0.47 mmol) in DME (10 mL) at −78 °C. The low-temperature bath was removed and the suspension was stirred at room temperature for 45 min. Then, Me_3SiCl (0.20 mL, 1.55 mmol) was added at −78 °C. After addition of Me_3SiCl, the suspension was stirred at room temperature for 3 h and filtered and the solution evaporated to dryness. The residue was dissolved in MeOH (0.5 mL) and an aqueous solution of CsCl (200 mg, 20 mL) was added dropwise to give a red solid. The solid was washed with H_2O (2×15 mL) and hexane (2× 15 mL) to afford Cs-**7** (yield: 254 mg, 90%). Alternatively, [NMe_4]-**7** can be isolated in 95% yield, by the addition of an aqueous solution of [NMe_4]Cl. Red crystals suitable for an X-ray diffraction study were grown by slow evaporation of a solution of [NMe_4]-**7** in acetone at room temperature. ^1H NMR: $\delta=4.19$ (brs, 0.66H; C_c-*H*), 3.77 (brs, 1.33H; C_c-*H*), 0.33 (s, 6H; Si-CH_3), 0.30 ppm (s, 12H; Si-CH_3); $^{13}C\{^1H\}$ NMR: $\delta=55.84$ (C_c-H), 54.56 (C_c-H), 51.96 (C_c-H), 46.85 (C_c-Si), 3.20 ppm (Si-CH_3); ^{11}B NMR: $\delta=8.25$ (d, $^1J(H,B)=140$ Hz, 2B), 3.71 (d, $^1J(H,B)=141$ Hz, 2B), −2.45 (d, $^1J(H,B)=126$ Hz, 4B), −5.44 (d, $^1J(H,B)=119$ Hz, 2B), −6.52 (d, $^1J(H,B)=123$ Hz, 2B), −11.59 (d, $^1J(H,B)=172$ Hz, 1B), −13.42 (d, $^1J(H,B)=158$ Hz, 2B), −15.09 (d, $^1J(H,B)=156$ Hz, 1B), −19.66 ppm (d, $^1J(H,B)=177$ Hz, 2B); $^{29}Si\{^1H\}$ NMR: $\delta=10.75$ ppm; IR: $\tilde{\nu}=3055$ (C_c–H), 2561 (B–H), 1250 cm^{-1} (Si–CH_3); MALDI-TOF-MS: *m/z* calcd for $[M-Cs]^-$: 468.42; found: 467.3; elemental analysis calcd (%) for $C_{10}H_{38}B_{18}CoCsSi_2$ (601): C 19.98, H 6.37; found: C 20.49, H 6.48.

Synthesis of [NMe$_4$][8,8′-μ-(1″,2″-C$_6$H$_4$)-1,1′-μ-SiMe$_2$-3,3′-Co(1,2-C$_2$B$_9$H$_9$)$_2$] ([NMe$_4$]-8): The procedure was similar to that used to prepare Cs-**4**, with Cs-**2** (95 mg, 0.18 mmol) in DME (5 mL)at −78 °C, *n*BuLi (0.12 mL, 0.19 mmol) and Me_2SiHCl (40 μL, 0.35 mmol). After addition of Me_2SiHCl, the suspension was stirred at room temperature for 3 h, and subsequently filtered and evaporated to dryness. The residue was dis-

solved in MeOH (0.1 mL) and an aqueous solution of $[NMe_4]Cl$ (25 mg, 5 mL) was added dropwise to give a red solid. The solid was washed with H_2O (2×10 mL) and hexane (2× 10 mL). The resultant solid was purified from a solution of CH_2Cl_2 to afford $[NMe_4]$-**8** (yield: 92 mg, 77%). ^{1}H NMR: δ=6.78 (s, 4H; C_6H_4), 3.48 (br s, 2H; C_c-H), 3.35 (s, 12H, N-CH_3), 0.39 (s, 3H, Si-CH_3), 0.25 ppm (s, 3H, Si-CH_3); ^{13}C{^{1}H} NMR: δ=128.98 (C_6H_4), 124.83 (C_6H_4), 55.11 (N-CH_3), 49.67 (C_c-H), 36.73 (C_c-Si), −4.46 (Si-CH_3), −5.84 ppm (Si-CH_3); ^{11}B NMR: δ=25.93 (s, 2B), 2.41 (d, ^1J(H,B)= 131 Hz, 3B), 1.69 (d, ^1J(H,B)=75 Hz, 3B), −2.98 (d, ^1J(H,B)=131 Hz, 4B), −11.76 (d, ^1J(H,B)=147 Hz, 4B), −24.51 ppm (d, ^1J(H,B)=161 Hz, 2B); ^{29}Si{^{1}H} NMR: δ=11.74 ppm; IR: $\tilde{\nu}$= 3034 (C_c–H), 2975 (C_{aryl}–H), 2954, 2923, 2561 (B–H), 1481 (C–N), 1254 cm^{-1} (Si–CH_3); MALDI-TOF-MS: *m/z* calcd for $[M-NMe_4]^-$: 454.3; found: 454.3; elemental analysis calcd (%) for $C_{16}H_{40}B_{18}CoNSi$: C 30.97, H 6.35 N 2.01; found: C 29.76, H 6.48, N 1.99.

Synthesis of Cs[8,8′-μ-(1″,2″-C_6H_4)-1,1′-μ-SiMeH-3,3′-Co(1,2-$C_2B_9H_9$)$_2$] (Cs-9): The procedure was similar to that used to prepare Cs-**5**, with Cs-**2** (373 mg, 0.70 mmol) in DME (9 mL) at −78°C, *n*BuLi (0.90 mL, 1.44 mmol) and CH_3SiHCl_2 (0.15 mL, 1.42 mmol). After addition of CH_3SiHCl_2, the suspension was stirred at room temperature for 3 h and subsequentely filtered and the solution evaporated to dryness. The resultant residue was dissolved in MeOH, and an aqueous solution of $[NMe_4]Cl$ was added to give $[NMe_4]$-**9** (yield 60%). Furthermore, Cs-**9** can be isolated from the addition of an aqueous solution of CsCl in a 65% yield. ^{1}H NMR: δ=6.76 (s, 4H; C_6H_4), 5.25 (q, ^3J(H,H)=3.4 Hz, 0.24H; Si-H), 4.97 (q, ^3J(H,H)=3.4 Hz, 0.76H; Si-H), 3.61 (br s, 2H; C_c-H), 0.48 (d, ^3J(H,H)=3.4 Hz, 2.28H,; Si-CH_3), 0.38 ppm (d, ^3J(H,H)= 3.4 Hz, 0.72H; Si-CH_3); ^{13}C{^{1}H} NMR: δ=128.96, 124.84 (C_6H_4), 50.84 (C_c-H), 48.56 (C_c-H), 32.30 (C_c-Si), 31.88 (C_c-Si),-6.32 (Si-CH_3), −6.87 ppm (Si-CH_3); ^{11}B NMR: δ=27.47 (s, 2B), 2.56 (d, ^1J(H,B)= 131 Hz; 6B), −2.73 (d, ^1J(H,B)=122 Hz; 4B), −11.55 (d, ^1J(H,B)= 132 Hz; 4B), −24.04 ppm (d, ^1J(H,B)=144 Hz, 2B); ^{29}Si{^{1}H} NMR: δ= 2.69 ppm; IR: $\tilde{\nu}$=3036 (C_c–H), 2970 (C_{aryl}–H), 2577 (B–H), 2162 (Si–H), 1257 cm^{-1} (Si–CH_3); MALDI-TOF-MS: *m/z* calcd for $[M-Cs]^-$: 440.3; found: 440.2; elemental analysis calcd (%) for $C_{11}H_{26}B_{18}CoSiCs$ (572.8): C 23.06, H 4.57; found: C 22.96, H 5.00.

Synthesis of $[NMe_4]$[8,8′-μ-(1″,2″-C_6H_4)-1-$SiMe_3$-3,3′-Co(1,2-$C_2B_9H_9$)-(1′,2′-$C_2B_9H_{10}$)] ($[NMe_4]$-10): The procedure was similar to that used to prepare Cs-**7**, with Cs-**2** (100 mg, 0.19 mmol) in DME (5 mL) at −78°C, *n*BuLi (0.25 mL, 0.40 mmol) and Me_3SiCl (0.10 mL, 0.77 mmol). After addition of Me_3SiCl, the suspension was stirred at room temperature for 3 h. The suspension was filtered and the solution evaporated to dryness. The residue was dissolved in MeOH (0.1 mL) and a solution of $[NMe_4]Cl$ (25 mg, 5 mL) in water was added dropwise to give a red solid. The solid was washed with H_2O (2×10 mL) and hexane (2×10 mL) and recrystallised from acetone to afford $[NMe_4]$-**10** (yield: 72 mg, 69%). ^{1}H NMR: δ=6.78 (s, 4H; C_6H_4), 3.52 (br s, 2H; C_c-H), 3.45 (br s, 1H; C_c-H), 3.28 (s, 12H; N-CH_3), 0.28 ppm (s, 9H; Si-CH_3); ^{13}C{^{1}H} NMR: δ=128.86, 128.56, 125.16 (C_6H_4), 55.12 (N-CH_3), 50.12 (C_c-H), 49.84 (C_c-H), 42.11 (C_c-H), 41.06 (C_c-Si), 0.10 ppm (Si-CH_3); ^{11}B NMR: δ=26.50 (s, 1B), 24.50 (s, 1B), 1.06 (2B), −1.46 (2B), −2.58 (2B), −4.64 (2B), −5.67 (2B), −10.80 (1B), −11.96 (1B), −13.67 (2B), −23.64 (d, ^1J(H,B)= 155 Hz; 1B), −25.00 ppm (d, ^1J(H,B)=155 Hz; 1B); ^{29}Si{^{1}H} NMR: δ= 8.63 ppm; IR: $\tilde{\nu}$=3036 (C_c–H), 2954 (C_{aryl}–H), 2584 (B–H), 1481 (C–N), 1253 cm^{-1} (Si–CH_3); MALDI-TOF-MS: *m/z* calcd for $[M-NMe_4]^-$: 470.39; found: 469.17; elemental analysis calcd (%) for $C_{17}H_{44}B_{18}CoNSi{\cdot}Me_2CO$: C 39.88, H 8.37, N 2.33; found: C 39.64, H 8.28, N 2.32.

Table 6. Crystallographic data for $[NMe_4]$-**3**, $[NMe_4]$-**4** and $[NMe_4]$-**7** at −100°C.

	$[NMe_4]$-**3**	$[NMe_4]$-**4**	$[NMe_4]$-**7**
empirical formula	$C_{10}H_{40}B_{18}CoNSi$	$C_{10}H_{38}B_{18}CoNSi$	$C_{14}H_{50}B_{18}CoNSi_2$
M_r	456.03	0454.01	542.24
crystal system	monoclinic	monoclinic	monoclinic
crystal shape/colour	plate/yellow	plate/red	plate/red
space group	$P2_1/c$ (no. 14)	$P2_1/m$ (no. 11)	$C2/c$ (no. 15)
a [Å]	7.1294(5)	7.3092(3)	15.9542(6)
b [Å]	30.456(2)	13.7910(11)	14.6275(6)
c [Å]	11.5788(7)	13.6504(8)	13.1513(4)
β [°]	91.206(4)	104.204(3)	98.714(2)
V [Å^3]	2513.6(3)	1237.19(14)	3033.69(19)
Z	4	2	4
ρ [g cm^{-3}]	1.205	1.219	1.187
μ [cm^{-1}]	7.32	7.43	6.54
goodness-of-fit[a]	1.084	1.042	1.029
R[b] [$I>2\sigma(I)$]	0.0949	0.0733	0.0524
R_w[c] [$I>2\sigma(I)$]	0.1646	0.1591	0.1042

[a] $S=[\Sigma(w(F_o^2-F_c^2)]/(n-p)^{1/2}$. [b] $R=\Sigma||F_o|-|F_c||/\Sigma|F_o|$. [c] $R_w=[\Sigma w(|F_o^2|-|F_c^2|)^2/\Sigma w|F_o^2|^2]^{1/2}$.

X-ray diffraction studies—structure determinations of $[NMe_4]$-3, $[NMe_4]$-4 and $[NMe_4]$-7: Single-crystal data collections for $[NMe_4]$-**3**, $[NMe_4]$-**4** and $[NMe_4]$-**7** were performed at −100°C on an Enraf Nonius KappaCCD diffractometer with graphite monochromatised $Mo_{K\alpha}$ radiation (λ=0.71073 Å). A total of 4538, 2499 and 2976 unique reflections were collected for $[NMe_4]$-**3**, $[NMe_4]$-**4** and $[NMe_4]$-**7**, respectively. Crystallographic data are presented in Table 6. The structures were solved by direct methods and refined on F^2 by the SHELX-97 program.[22] For each structure, the carbon and boron atoms could be reliably distinguished.

For $[NMe_4]$-**3**, non-hydrogen atoms were refined with anisotropic thermal displacement parameters and hydrogen atoms were treated as riding atoms using the SHELX-97 default parameters. *R* values were fairly high because of the high mosaicity of the crystals.

For $[NMe_4]$-**4**, the cobaltabis(dicarbollide) anion had a crystallographic mirror symmetry with the cobalt, silicon and methyl carbon atoms lying at the symmetry element. The $[NMe_4]^+$ ion was disordered in two orientations with the partially occupied nitrogen atom and the two partially occupied methyl carbon atoms of each orientation lying in the mirror plane. The cation was refined as a rigid group, but as refinement of the site occupation parameters did not converge well, the parameters were fixed to 0.6 and 0.4. Non-hydrogen atoms of the anion were refined with anisotropic thermal displacement parameters, but those of the disordered cation were refined with isotropic displacement parameters. All hydrogen atoms were treated as riding atoms using the SHELX-97 default parameters.

For $[NMe_4]$-**7**, the cobaltabis(dicarbollide) anion had a crystallographic twofold symmetry with the cobalt atom lying at the symmetry element. The $[NMe_4]^+$ ion was disordered in two orientations with the partially occupied nitrogen atom lying at the vicinity of the twofold axis. The cation was refined as a rigid group. All non-hydrogen atoms were refined with anisotropic thermal displacement parameters and the hydrogen atoms were treated as riding atoms using the SHELX-97 default parameters.

CCDC-659301 ($[NMe_4]$-**3**), 652272 ($[NMe_4]$-**4**) and 652273 ($[NMe_4]$-**7**) contain the supplementary crystallographic data for this paper. These data can be obtained free of charge from The Cambridge Crystallographic Data Centre via www.ccdc.cam.ac.uk/data_request/cif.

Calculation details: Geometries of the compounds were optimised with the B3LYP hybrid functional[23] and the 6-311G(d,p) basis for all elements. Unless otherwise noted, energies are reported at this level. Natural population analysis was performed at the same level. Transition states were found at the B3LYP/6-31G level, characterised by a single imaginary frequency, and visualisation of the corresponding vibrational modes ensured that the desired minima are connected. Magnetic shieldings were computed for optimised geometries by employing gauge-including atomic orbitals (GIAOs)[21] with the B3LYP hybrid functional together with the

basis 6-31++G(d). The ^{11}B chemical shifts were calculated relative to B_2H_6 and converted to the usual $BF_3{\cdot}OEt_2$. These combinations of functional and basis set gave good results, for more exhaustive calculations on cobaltacarboranes see Bühl et al.[19] All computations were performed with the Gaussian 03 program.[24]

Acknowledgements

This work has been supported by MEC, MAT 2006—05339 and Generalitat de Catalunya, 2005/SGR/00709. E.J.J.-P. thanks MEC for a FPU grant.

[1] I. B. Sivaev, V. I. Bregadze, *Collect. Czech. Chem. Commun.* **1999**, *64*, 783.
[2] a) L. Ma, J. Hamdi, M. F. Hawthorne, *Inorg. Chem.* **2005**, *44*, 7249; b) P. Matejicek, P. Cigler, K. Procházka, V. Kral, *Langmuir* **2006**, *22*, 575; c) G. Chevrot, R. Schurhammer, G. Wipff, *J. Phys. Chem. B* **2006**, *110*, 9488.
[3] J. Plesek, *Chem. Rev.* **1992**, *92*, 269.
[4] a) S. H. Strauss, *Chem. Rev.* **1993**, *93*, 927; b) C. A. Reed, *Acc. Chem. Res.* **1998**, *31*, 133.
[5] a) C. Masalles, S. Borrós, C. Viñas, F. Teixidor, *Adv. Mater.* **2000**, *12*, 1199; b) C. Masalles, J. Llop, C. Viñas, F. Teixidor, *Adv. Mater.* **2002**, *14*, 826; c) S. Gentil, E. Crespo, I. Rojo, A. Friang, C. Viñas, F. Teixidor, B. Grüner, D. Gabel, *Polymer* **2005**, *46*, 12218.
[6] a) C. Viñas, S. Gómez, J. Bertran, F. Teixidor, J.-F. Dozol, H. Rouquette, *Chem. Commun.* **1998**, 191; b) C. Viñas, S. Gómez, J. Bertran, F. Teixidor, J.-F. Dozol, H. Rouquette, *Inorg. Chem.* **1998**, *37*, 3640; c) B. Grüner, J. Plesek, J. Baca, I. Cisarova, J.-F. Dozol, H. Rouquette, C. Viñas, P. Selucky, J. Rais, *New J. Chem.* **2002**, *26*, 1519.
[7] M. F. Hawthorne, A. Maderna, *Chem. Rev.* **1999**, *99*, 3421.
[8] a) J. N. Francis, M. F. Hawthorne, *Inorg. Chem.* **1971**, *10*, 594; b) J. Plesek, S. Hermanek, K. Base, L. J. Todd, W. F. Wright, *Collect. Czech. Chem. Commun.* **1976**, *41*, 3509; c) Z. Janousek, J. Plesek, S. Hermanek, K. Base, L. J. Todd, W. F. Wright, *Collect. Czech. Chem. Commun.* **1981**, *46*, 2818; d) L. Matel, F. Mascasek, P. Rajec, S. Hermanek, J. Plesek, *Polyhedron*, **1982**, *1*, 511.
[9] a) P. Selucky, J. Plesek, J. Rais, M. Kyrs, L. Kadlecova, *J. Radioanal. Nucl. Chem.* **1991**, *149*, 131; b) J. Plesek, S. Hermanek, *Collect. Czech. Chem. Commun.* **1995**, *60*, 1297; c) P. K. Hurlburt, R. L. Miller, K. D. Abney, T. M. Foreman, R. J. Butcher, S. A. Kinkead, *Inorg. Chem.* **1995**, *34*, 5215; d) J. C. Fanning, L. A. Huff, W. A. Smith, A. S. Terell, L. Yasinsac, L. J. Todd, S. A. Jasper, D. J. McCabe, *Polyhedron* **1995**, *14*, 2893; e) M. D. Mortimer, C. B. Knoble, M. F. Hawthorne, *Inorg. Chem.* **1996**, *35*, 5750; f) A. Franken, J. Plesek, C. Nachtigal, *Collect. Czech. Chem. Commun.* **1997**, *62*, 746; g) J. Plesek, S. Hermanek, A. Franken, I. Cisarova, C. Nachtigal, *Collect. Czech. Chem. Commun.* **1997**, *62*, 47; h) J. Plesek, B. Grüner, J. Báca, J. Fusek, I. Cisarová, *J. Organomet. Chem.* **2002**, *649*, 181; i) J. Plesek, B. Grüner, I. Cisarová, J. Báca P. Selucky, J. Rais, *J. Organomet. Chem.* **2002**, *657*, 59; j) I. Rojo, F. Teixidor, C. Viñas, R. Kivekäs, R. Sillanpää, *Chem. Eur. J.* **2003**, *9*, 4311; k) I. Rojo, F. Teixidor, R. Kivekäs, R. Sillanpää, C. Viñas, *J. Am. Chem. Soc.* **2003**, *125*, 14720; l) F. Teixidor, J. Pedrajas, I. Rojo, C. Viñas, R. Kivekäs, R. Sillanpää, I. Sivaev, V. Bregadze, S. Sjöberg, *Organometallics* **2003**, *22*, 3414; m) B. Grüner, L. Mikulasek, J. Báca, I. Cisarova, V. Bohmer, C. Danila, M. M. Reinoso-Garcia, W. Verboom, D. N. Reinhoudt, A. Casnati, R. Ungaro. *Eur. J. Org. Chem.* **2005**, 2022.
[10] a) R. M. Chamberlin, B. L. Scott, M. M. Melo, K. D. Abney, *Inorg. Chem.* **1997**, *36*, 809; b) S. A. Fino, K. A. Benwitz, K. M. Sullivan, D. L. LaMar, K. M. Stroup, S. M. Giles, G. J. Balaich, R. M. Chamberlin, K. D. Abney, *Inorg. Chem.* **1997**, *36*, 4604.
[11] I. Rojo, F. Teixidor, C. Viñas, R. Kivekäs, R. Sillanpää, *Chem. Eur. J.* **2004**, *10*, 5376.
[12] a) R. Núñez, A. González, C. Viñas, F. Teixidor, R. Sillanpää, R. Kivekäs, *Org. Lett.* **2005**, *7*, 231; b) R. Núñez, A. González-Campo, C. Viñas, F. Teixidor, R. Sillanpää, R. Kivekäs, *Organometallics* **2005**, *24*, 6351; c) R. Núñez, A. González-Campo, A. Laromaine, F. Teixidor, R. Sillanpää, R. Kivekäs, C. Viñas, *Org. Lett.* **2006**, *8*, 4549; d) A. González-Campo, R. Núñez, F. Teixidor, C. Viñas, R. Sillanpää, R. Kivekäs, *Macromolecules* **2007**, *40*, 5644.
[13] T. Venable, W. Hutton, R. Grimes, *J. Am. Chem. Soc.* **1984**, *106*, 29.
[14] I. Rojo, F. Teixidor, R. Kivekäs, R. Sillanpää, C. Viñas, *Organometallics* **2003**, *22*, 4642.
[15] a) M. F. Hawthorne, D. C. Young, T. D. Andrews, D. V. Howe, R. L. Pilling, A. D. Pitts, M. Reintjes, L. F. Warren, Jr., Patrick, A. Wegner, *J. Am. Chem. Soc.* **1968**, *90*, 879; b) L. Matel, F. Macasek, P. Rajec, S. Hermanek, J. Plesek, *Polyhedron* **1982**, *1*, 511; c) H. Horáková, R. Vespalec, *Spectrochim. Acta Part A* **2006**, *65*, 378.
[16] a) R. Bauernschmitt, R. Ahlrichs, *Chem. Phys. Lett.* **1996**, *256*, 454; b) R. E. Stratmann, G. E. Scuseria, M. J. Frisch, *J. Chem. Phys.* **1998**, *109*, 8218.
[17] M. F. Hawtorne, J. I. Zink, J. M. Skelton, M. J. Bayer, C. Liu, E. Livshits, R. Baer, D. Neuhauser, *Science* **2004**, *303*, 1849.
[18] a) J. Llop, C. Viñas, F. Teixidor, L. Victori, R. Kivekäs, R. sillanpää, *Organometallics* **2002**, *21*, 355; b) R. Núñez, O. Tutusaus, F. Teixidor, C. Viñas, R. Sillanpää, R. Kivekäs, *Chem. Eur. J.* **2005**, *11*, 5637.
[19] M. Bühl, D. Hnyk, J. Machácek, *Chem. Eur. J.* **2005**, *11*, 4109.
[20] R. Custelcean, J. E. Jackson, *Chem. Rev.* **2001**, *101*, 1963.
[21] a) R. Ditchfield, *Mol. Phys.* **1974**, *27*, 789; b) K. Wolinski, J. F. Hinton, P. Pulay, *J. Am. Chem. Soc.* **1990**, *112*, 8251; c) GIAO-DFT implementation: J. R. Cheeseman, G. W. Trucks, T. A. Keith, M. J. Frisch, *J. Chem. Phys.* **1996**, *104*, 5497.
[22] G. M. Sheldrick, SHELX-97, University of Göttingen, Germany, **1997**.
[23] a) A. D. Becke *J. Chem. Phys.* **1993**, *98*, 5648; b) C. Lee, W. Yang, R. G. Parr, *Phys. Rev. B* **1988**, *37*, 785.
[24] Gaussian 03 (Revision BO.1), M. J. Frisch, G. W. Trucks, H. B. Schlegel, G. E. Scuseria, M. A. Robb, J. R. Cheeseman, J. A. Montgomery, Jr., T. Vreven, K. N. Kudin, J. C. Burant, J. M. Millam, S. S. Iyengar, J. Tomasi, V. Barone, B. Mennucci, M. Cossi, G. Scalmani, N. Rega, G. A. Petersson, H. Nakatsuji, M. Hada, M. Ehara, K. Toyota, R. Fukuda, J. Hasegawa, M. Ishida, T. Nakajima, Y. Honda, O. Kitao, H. Nakai, M. Klene, X. Li, J. E. Knox, H. P. Hratchian, J. B. Cross, C. Adamo, J. Jaramillo, R. Gomperts, R. E. Stratmann, O. Yazyev, A. J. Austin, R. Cammi, C. Pomelli, J. W. Ochterski, P. Y. Ayala, K. Morokuma, G. A. Voth, P. Salvador, J. J. Dannenberg, V. G. Zakrzewski, S. Dapprich, A. D. Daniels, M. C. Strain, O. Farkas, D. K. Malick, A. D. Rabuck, K. Raghavachari, J. B. Foresman, J. V. Ortiz, Q. Cui, A. G. Baboul, S. Clifford, J. Cioslowski, B. B. Stefanov, G. Liu, A. Liashenko, P. Piskorz, I. Komaromi, R. L. Martin, D. J. Fox, T. Keith, M. A. Al-Laham, C. Y. Peng, A. Nanayakkara, M. Challacombe, P. M. W. Gill, B. Johnson, W. Chen, M. W. Wong, C. Gonzalez, J. A. Pople, Gaussian, Inc., Pittsburgh PA, **2004**.

Received: December 20, 2007
Published online: April 11, 2008

